Clim Dyn (2013) 41:2617–2642
DOI 10.1007/s00382-013-1752-6

Asian monsoon simulations by Community Climate Models CAM4 and CCSM4

Siraj ul Islam · Youmin Tang · Peter L. Jackson

Received: 21 July 2012 / Accepted: 25 March 2013 / Published online: 5 April 2013

Abstract This study examines the ability of Community Atmosphere Model (CAM) and Community Climate System Model (CCSM) to simulate the Asian summer monsoon, focusing particularly on inter-model comparison and the role of air–sea interaction. Two different versions of CAM, namely CAM4 and CAM5, are used for uncoupled simulations whereas coupled simulations are performed with CCSM4 model. Ensemble uncoupled simulations are performed for a 30 year time period whereas the coupled model is integrated for 100 years. Emphasis is placed on the simulation of monsoon precipitation by analyzing the interannual variability of the atmosphere-only simulations and sea surface temperature bias in the coupled simulation. It is found that both CAM4 and CAM5 adequately simulated monsoon precipitation, and considerably reduced systematic errors that occurred in predecessors of CAM4, although both tend to overestimate monsoon precipitation when compared with observations. The onset and cessation of the precipitation annual cycle, along with the mean climatology, are reasonably well captured in their simulations. In terms of monsoon interannual variability and its teleconnection with SST over the Pacific and Indian Ocean, both CAM4 and CAM5 showed modest skill. CAM5, with revised model physics, has significantly improved the simulation of the monsoon mean climatology and showed better skill than CAM4. Using idealized experiments with CAM5, it is seen that the adoption of new boundary layer schemes in CAM5 contributes the most to reduce the monsoon overestimation bias in its simulation. In the CCSM4 coupled simulations, several aspects of the monsoon simulation are improved by the inclusion of air–sea interaction, including the cross-variability of simulated precipitation and SST. A significant improvement is seen in the spatial distribution of monsoon mean climatology where a too-heavy monsoon precipitation, which occurred in CAM4, is rectified. A detailed investigation of this significant precipitation reduction showed that the large systematic cold SST errors in the Northern Indian Ocean reduces monsoon precipitation and delays onset by weakening local evaporation. Sensitivity experiments with CAM4 further confirmed these results by simulating a weak monsoon in the presence of cold biases in the Northern Indian Ocean. It is found that although the air–sea coupling rectifies the major weaknesses of the monsoon simulation, the SST bias in coupled simulations induces significant differences in monsoon precipitation. The overall simulation characteristics demonstrate that although the new model versions CAM4, CAM5 and CCSM4, are significantly improved, they still have major weaknesses in simulating Asian monsoon precipitation.

S. u. Islam · Y. Tang (✉) · P. L. Jackson
Environmental Science and Engineering, University of Northern British Columbia, 3333 University way, Prince George, BC V2N 4Z9, Canada
e-mail: ytang@unbc.ca

1 Introduction

The monsoon is one of the most prominent and dynamic phenomena of the climate system, and has a large effect on weather and climate anomalies at both local and global scales. Monsoon systems are caused by the seasonal reversal of winds due to differential heating between land and ocean, and result in seasonal heavy precipitation patterns. The dominant monsoon systems around the globe are the Asian, Australian, African and American monsoons. Among these various monsoon systems, the Asian summer monsoon composed of the East Asian monsoon (EAM) and

the South Asian monsoon (SAM) (Lau and Li 1984) receives the heaviest seasonal precipitation during the summer months and has a major impact on global atmospheric circulations. The SAM region includes parts of the Arabian Sea, the Indian continent and the Bay of Bengal (Goswami et al. 1999); the region receives around 75 % of its annual precipitation during the summer season in the months of June, July, August and September (JJAS). Complex topographic features such as the Himalayas (in the north and north east) and the Western Ghats (along the western coast of India) strongly influence the monsoon circulations. Any monsoon fluctuations are often associated with floods, droughts, and other climatic extreme events in the region (Malik et al. 2010). The SAM precipitation has a very strong temporal and spatial variation due to the interaction between regional topography and the monsoon circulation. A detailed understanding of the different external forcing mechanisms that modulate the SAM precipitation is therefore necessary for the societal and economical needs of the South Asian region. The study of the SAM variability and its prediction is challenging and important issue in the scientific community.

Climate models have been significantly improved in simulating the mean global climate (Randall et al. 2007) and in predicting climate anomalies at the seasonal time scale (Liang et al. 2009; Lee et al. 2010; Kang et al. 2002; Kang and Shukla 2006; Wang et al. 2004). These models are fairly good at simulating the average atmospheric state and large scale patterns, but poor at simulating relatively small and local atmospheric systems such as the monsoon. In some of the studies such as Kang et al. (2004) and Wang et al. (2004), it has been seen that even when forced with observed sea surface temperatures (SSTs), Global Climate Model (GCM) performance over the SAM region is not satisfactory and presents large systematic biases. Even in coupled Atmosphere Ocean Global Climate Models (AOGCMs), which are believed to simulate the most realistic physical processes, there are notable biases in simulation of the mean climate and its variability (Covey et al. 2003; Meehl et al. 2005). These discrepancies include a Pacific cold bias, a double Intertropical Convergence Zone (ITCZ), and a westward shift of El Nino–Southern Oscillation (ENSO) variability (AchutaRao and Sperber 2006; Covey et al. 2000; Joseph and Nigam 2006). Gimeno et al. (2010) have shown the Northern Indian Ocean, particularly the Arabian Sea, to be an important moisture source for SAM and any changes in Indian Ocean SSTs affect monsoon precipitation by altering the amount of moisture available for transport towards South Asia. Furthermore, due to the strong air–sea coupling over the Indian Ocean, any variation in the strength of the SAM precipitation influences the SST variation which significantly complicates the detection of monsoon variability related to other changes in the lower boundary of the atmosphere in the coupled model.

It has been a challenging issue to correctly simulate the monsoon variability at seasonal and interannual time scales (Annamalai et al. 2007; Dai 2006; Kripalani et al. 2007; Lin 2007; Waliser et al. 2007) and the relationship between SST anomalies and SAM precipitation variability (Annamalai and Liu 2005; Meehl and Arblaster 2002; Shukla and Paolino 1983; Rasmusson and Carpenter 1983). An important issue is the simulation of the relationship between local SAM and SST variations in the Pacific and Indian Ocean. The link between the SAM precipitation and ENSO has been well documented in observations and modeling. For example, it has been reported that the warm phase (El Nino) is associated with weakening of the Indian monsoon and an overall reduction in precipitation, while the cold phase (La Nina) is associated with the strengthening of the Indian monsoon and an enhancement of precipitation (Kanamitsu and Krishnamurti 1978; Krishnamurti et al. 1989; Palmer et al. 1992; Pant and Parthasarathy 1981; Rasmusson and Carpenter 1983; Shukla and Paolino 1983; Shukla and Mooley 1987; Sikka 1999). Meehl et al. (2012), described SAM as a fully coupled air–sea–land system which can be better reproduced by AOGCMs. Many other studies also reported that AOGCMs perform better than atmosphere-only GCMs in simulating the SAM with moderate skill (Kumar et al. 2005; Wang et al. 2005).

As discussed above, an intensive research effort has been made to improve simulation of monsoon systems by climate models and significant progress has been made in recent years. Among these models, Community Climate Models developed at the US National Center for Atmospheric Research (NCAR) have played an important role in monsoon research due to their complete physical dynamics and easy implementation. NCAR released new versions of the climate models, i.e., the Community Atmosphere Model version 4 and version 5 (CAM4 and CAM5) and the Community Climate System Model version 4 (CCSM4). In the recent paper by Meehl et al. (2012) documenting the monsoon simulations in the Community Climate Model version 4 (CCSM4), the SAM and Australian monsoon is thoroughly examined for the fully coupled model. They also compared the CAM4 atmosphere simulation with coupled run and discussed the improvement of CCSM4 compared with the previous generation of this model (CCSM3) in simulating the monsoon. Also in the study by Meehl et al. (2006), the monsoon in CCSM3 was described and compared to a previous version of the model simulation (Meehl and Arblaster 1998). In this context, it is of interest and importance to evaluate the ability of these new model versions, particularly CAM5, in simulating the monsoon. The important factors affecting monsoon–SST

relationships, such as air–sea coupling and SST bias from the CCSM4, need to be studied in detail to determine the strengths and weaknesses of these new models. A systematic evaluation is also important if these new model versions are to be used for seasonal climate prediction or climate change studies. In this study, we therefore explore in detail the strengths and limitations of CAM4, CAM5 and CCSM4 in simulating SAM precipitation with an emphasis on the mean climate, seasonal and interannual variability and the relationship between SAM and SST (local and remote) in the simulations. Our focus is (1) on the analysis of SAM interannual variability when simulations are forced with observed SST and (2) the role of air–sea coupling and SST bias in simulating the SAM. In the latter, using sensitivity experiments, we also examine the effect of Northern Indian SST bias in coupled simulations and its impact on SAM.

This paper is organized as follows. Section 2 describes models, data and experiments. Section 3 investigates the mean climatology, annual cycle and evaluates simulated monsoon interannual variability in CAM4 and CAM5. Section 4 highlights and compares the coupled simulations of CAM4 (CCSM4) in terms of the mean climatology and SAM–SST relationship as well as the effect and importance of air–sea coupling over the SAM region. To address the effect of CCSM4 SST bias on the SAM precipitation, Sect. 5 explores results of sensitivity experiments followed by summary and conclusions in Sect. 6.

2 Models, experiments and validations

2.1 Models

Simulations are performed using the CAM4, CAM5 and CCSM4 models. These models are the latest in a succession of GCMs and AOGCMs that have been made widely available to the scientific community from NCAR. For the convenience of the reader we briefly introduce each model, but refer interested readers to the cited references for full details of each model.

CAM4 (Neale et al. 2010a) is developed from CAM3 (Collins et al. 2006a, b) with modifications to the deep convection (Neale et al. 2008), polar filtering (Anderson et al. 2009), and the polar cloud fraction in extremely cold conditions parameterization schemes (Vavrus and Waliser 2008). It uses an updated convection parameterization scheme (Neale et al. 2008; Richter and Rasch 2008). This model can be used with three different dynamic schemes (an Eulerian spectral scheme, a semi-Lagrangian scheme and a finite volume scheme) along with different resolution settings. CAM5 (Neale et al. 2010b) is modified significantly compared to CAM4, with a range of improvements in the representation of physical processes. It includes a new shallow convection scheme (Park and Bretherton 2009), a stratiform cloud microphysical scheme (Morrison and Gettelman 2008), an updated radiation scheme (Iacono et al. 2008) and 3-mode modal aerosol scheme (MAM3) (Liu et al. 2012).

The CCSM4 (Gent et al. 2011) coupled model descended from its predecessors, CCSM3 (Collins et al. 2006a, b) and CCSM2 (Kiehl and Gent 2004). It contains a new coupler that exchanges fluxes and state information among all the embedded models. These embedded models are the CAM4 atmospheric model, the Community Land Model (CLM4), the Los Alamos Parallel Ocean Program ocean model version 2.2 (POP 2.2) (Smith and Gent 2002) and the Community Ice Code version 4 (CICE4) sea ice model (Hunke and Lipscomb 2008). The CLM4 model operates on the same grids as the CAM4 model whereas CICE4 uses the same horizontal grid as POP 2.2, which has a displaced dipole grid (Smith and Kortas 1995).

2.2 Experimental design

A series of experiments are performed to achieve three goals: (1) exploring and comparing the ability of CAM4, CAM5 and CCSM4 in simulating the SAM; (2) evaluating the contribution of air–sea coupling to the simulation and (3) investigating the effect of SST bias on SAM precipitation. These experiments can be generally categorized as below:

1. *Control runs*: Thirty-two years (1978–2008) of uncoupled simulations are performed using the CAM4 and CAM5 atmospheric models forced with observed prescribed SST (HadSST, Reynolds et al. 2002) and sea ice data. Both models share the same 1.9° × 2.5° horizontal resolution using the finite volume (FV) dynamical core with 26 (in CAM4) and 30 (in CAM5[1]) vertical levels using a hybrid terrain-following coordinate system. Higher resolution simulation of CAM4 and CAM5 models are also performed using 0.9° × 1.25° in the horizontal for the same time period.
2. *Climatology run*: CAM4 is also run forced with the climatological (based on the observations from 1982 to 2001) seasonal cycle of SST and sea ice for 30 years. This is referred to as CAM4_CLIM.
3. *Coupled run*: In the case of the CCSM4 coupled experiment, a 100-year coupled integration is performed using present day climatological forcing. The

[1] CAM5 is run for different set of schemes. Standard run (control) of CAM5 has 30 vertical levels with all the default setting. The remaining set of CAM5 runs will be denoted with their particular name throughout the text.

output of the last 30 years of this coupled simulation is used.[2] In this simulation, the horizontal resolution of 1.9° × 2.5° and finite volume grids in both the atmospheric and land model is used, whereas the ocean and ice models share the same 1° × 1° resolution with a displaced pole grid. To facilitate comparison, observational datasets are interpolated to the resolution of model grids.

4. *Sensitivity runs*: Idealized experiments using different boundary forcings are performed with CAM4 and CAM5. Details of these experiments are given in the relevant sections.

Even a realistic model always contains random components and uncertainties such as those in boundary forcing or in initial conditions. To alleviate the impact of these random components and obtain a deterministic response of the model behavior to forcing (such as SST), an ensemble strategy is used for the above experiments except for the coupled run. For the control run, ensembles are constructed through perturbing the initial conditions, which allows us to separate the ''SST-forced'' (or external) response (Rowell et al. 1995). The perturbation of the initial conditions is performed by using the initial conditions lagged in time. For the climatology run, the same method is used to construct the ensembles. A detailed summary of all the experiments and the ensemble runs is given in Table 1. All simulation results from the control and climatology runs used for validation and presented in the next sections are the ensemble mean, unless otherwise indicated.

2.3 Validation

The following validation steps are used to examine the performance of the models in simulating the SAM monsoon: (1) the simulated SAM precipitation and wind by the CAM4 and CAM5 control runs are compared against the observed counterparts in terms of climatology, interannual variability, and the relationship to SST. (2) The climatological means from the CAM4 runs are compared against those from CCSM4 to explore the effects of ocean–atmosphere coupling on the SAM simulation. (3) To explore the impact of SST bias on monsoon simulations, CAM4 forced with a modified SST climatology that contain SST bias, is compared with that forced with the observed SST climatology (CAM4_CLIM).

The metrics and methods used to evaluate the simulations include mean bias, root means square error (RMSE), variance, correlation and regression analysis. In all the uncoupled simulations, the first year of the integration output is discarded as a spin-up time, which is considered sufficient for atmospheric-only simulations. In the case of coupled runs, the first 70 years are discarded as the ocean model needs more time for equilibration. Observed precipitation data from the Climate Prediction Center (CPC) Merged Analysis of Precipitation (CMAP; Xie and Arkin 1997), on a 2.5° × 2.5° grid, is used for validation of precipitation. The All-India Rainfall time series (AIR; Parthasarathy et al. 1995), which is a combination of 306 uniformly distributed station measurements, is also used in the analysis. National Centers for Environmental Prediction (NCEP; Kistler et al. 2001) reanalysis data, also on a 2.5° × 2.5° grid, are used to validate winds. Observed SST (HadSST) data (Reynolds et al. 2002) are used for coupled model SST validation.

3 Simulations by CAM4 and CAM5

We first examine ensemble mean simulations of CAM4 and CAM5 forced with prescribed observed SST and sea ice data. Before focusing on the SAM, we evaluate both models over the tropical region.

3.1 Climatological mean and seasonal cycle

The distribution of precipitation bias and root means square error (RMSE) is shown in Figs. 1 and 2 for the winter (December–February, DJF) and summer (June–September, JJAS) seasons. The whole tropical region is shown to assess overall model differences. Bias and RMSE are calculated by comparing model output data with observations (CMAP) for the time period 1979–2008.

The model bias for winter (DJF) precipitation simulations are shown in Fig. 1a and b for CAM4 and CAM5 respectively and their corresponding RMSE are shown in Fig. 1c, d. Significant large-scale spatial biases (Fig. 1a, b) over the equatorial Indian Ocean and Western Pacific Ocean, along with many regional biases, are found in the CAM4 and CAM5 simulations. The magnitude of these biases is higher in CAM4 whereas CAM5, to a large extent, significantly rectifies them in its simulation. Major improvements in the CAM5 simulation occur over the South African land areas where the precipitation overestimation seen in the CAM4 simulation is diminished. The RMSE patterns (Fig. 1c, d) further highlight the improved winter precipitation in the CAM5 simulation. In summer, when the precipitation activity over the northern hemisphere is enhanced, both models show biases in the form of excessive precipitation over the western Indian Ocean, central China, Himalayas, and in the subtropical Pacific Ocean (Fig. 2a, b). Over the eastern Indian Ocean, China Sea, central parts of Africa and in the west and east Pacific

[2] Subject to the computational conditions, the spin-up run was carried out 70 years, which basically allows atmospheric states to reach equilibrium.

Table 1 Summary of the experimental setups

Experiment name	Model used	Time period	Description/boundary conditions (BC)	No. of runs
CAM4	CAM4	1978–2008	1.9° × 2.5° horizontal resolution and 26 vertical levels. Prescribed observed SST data as BC	10
CAM5	CAM5	1978–2008	1.9° × 2.5° horizontal resolution and 30 vertical levels. Prescribed observed SST data as BC	10
CAM4_CLIM	CAM4	30 years	1.9° × 2.5° horizontal resolution and 26 vertical levels. Climatology SST data repeated each year	05
CCSM4	CCSM4	100 years	1.9° × 2.5° horizontal resolution and 26 vertical levels for CAM4 and 1° × 1° horizontal resolution with 60 vertical levels for POP2.2. Present day climatology forcing	01
CAM5_BAM	CAM5	1978–2008	1.9° × 2.5° horizontal resolution and 30 vertical levels with bulk aerosol model (BAM) scheme. Prescribed observed SST data as BC	01
CAM5_BAM_CAMRT	CAM5	1978–2008	1.9° × 2.5° horizontal resolution and 30 vertical levels with BAM and CAMRT (radiation) schemes. Prescribed observed SST data as BC	01
CAM5_BAM_HB	CAM5	1978–2008	1.9° × 2.5° horizontal resolution and 30 vertical levels with BAM and HB (Holtslag–Boville, boundary layer turbulence) schemes. Prescribed observed SST data as BC	01
CAM5_BAM_CAMRT_HB	CAM5	1978–2008	1.9° × 2.5° horizontal resolution and 30 vertical levels with BAM, HB, and CAMRT schemes. Prescribed observed SST data as BC	01
CAM4_POP	CAM4	1971–2000	Same as CAM4 but with predicted SST from CCSM4 climatology run	03
CAM4_AS_BoB	CAM4	1978–2000	Same as CAM4_CLIM but with climatology SST data modified in the AS and BoB region	03
CAM4_AS	CAM4	1978–2000	Same as CAM4_CLIM but with climatology SST data modified in the AS region only	03

CLIM climatology, *BC* boundary conditions, *AS* Arabian Sea, *BoB* Bay of Bengal

Ocean, the models underestimate precipitation. The spatial patterns of bias from both models are similar, but the magnitude of biases is higher in the CAM4 simulation whereas CAM5 is able to reduce many regional biases. Compared to the land, biases are significantly higher over the ocean. High magnitudes of RMSE (Fig. 2c, d) are seen over the northern Indian Ocean (Arabian Sea and Bay of Bengal) and the complex topography of the Himalayas. Similar to the winter, the summer RMSE of the CAM5 simulation is less than for the CAM4 simulation.

In general it is seen that, while both CAM4 and CAM5 are able to capture many observed features, they have regional biases somewhat similar to those in previous versions of these models (i.e., CAM3, reported in Meehl et al. 2006). In fact, these precipitation biases especially over the Indian and Pacific Oceans are probably an intrinsic error of the atmospheric model itself, as seen in Lin (2007) and our simulations. Compared to CAM4, the CAM5 simulation is improved with less regional bias.

The magnitudes of tropical two meter air temperature biases (not shown) in both CAM4 and CAM5 are small except in areas with complex topography such as the Himalayan region which is true for many climate models (IPCC 2007). Both models showed warm biases over most of the tropical domain. Larger errors are in regions of sharp elevation changes which may result simply from the mismatches between the models' smoothed topography and the actual topography.

As this paper mainly focuses on the Asian region, the rest of the analyses for CAM4 and CAM5 include only the Asian domain, and particularly discuss the SAM region (JJAS only). Figure 3 shows seasonal mean summer (JJAS) precipitation and 850 mb winds for (a) CAM4, (b) CAM5 and (c) observations (CMAP/NCEP). In the observations, there are two precipitation maxima, with heavier precipitation around the northern Indian Ocean and a weaker precipitation maximum along the equatorial Indian Ocean. This is an important characteristic of the SAM precipitation. Although both of these maxima are captured in the models, significant large-scale biases such as excessive precipitation over the Arabian Bay and diminished precipitation in the central and the eastern Indian Ocean extending into the Bay of Bengal is seen. Simulations also show reduced precipitation along the coast of Bangladesh and excessive rain over the Western Ghats of India. CAM4 simulates excessive precipitation in the eastern Arabian Sea and in the Bay of Bengal, with the maximum center around the Bay of Bengal shifted to the west of the observed maximum center. This is also true for the CAM5 simulation but the spatial magnitude of the precipitation is reduced bringing its climatology close to the observation. This same conclusion regarding the CAM4 simulation is

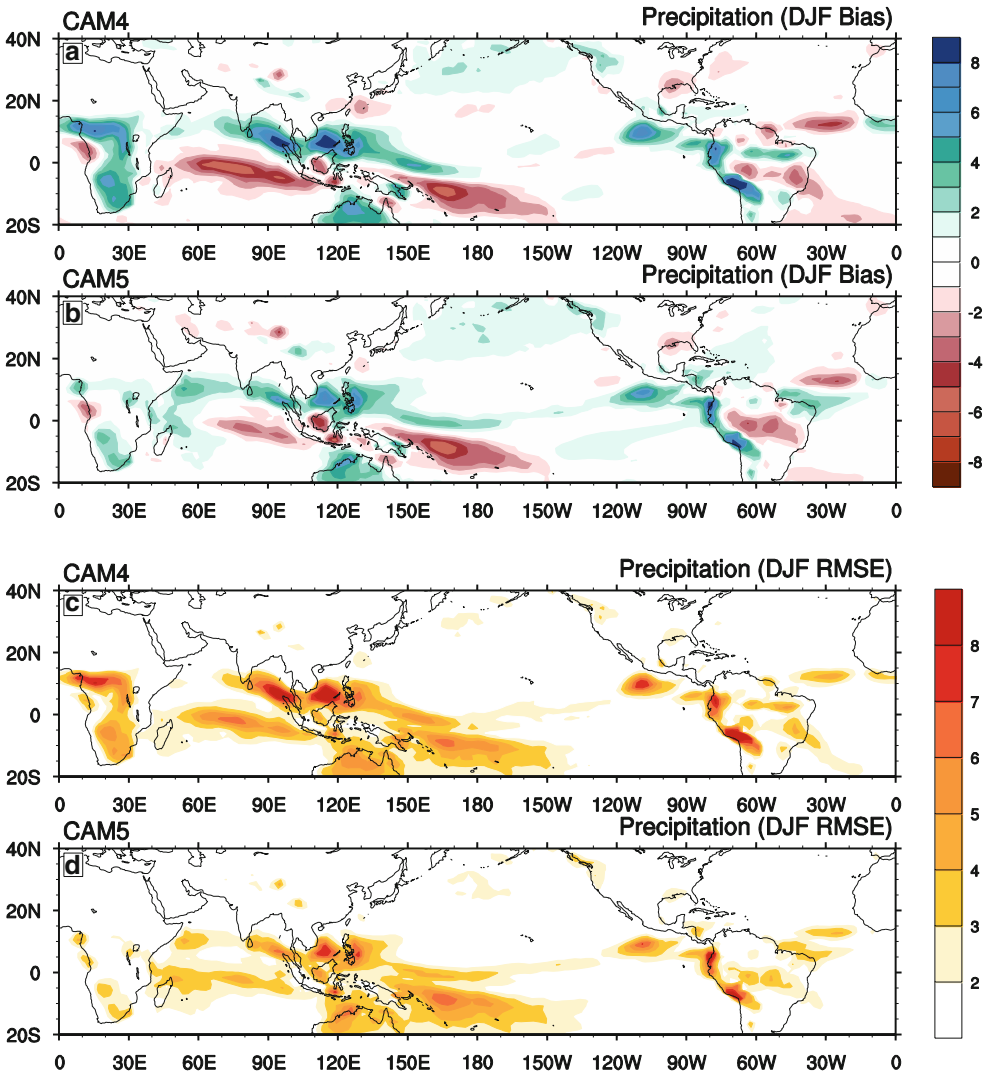

Fig. 1 Seasonal mean (December–February; DJF) precipitation differences (biases) and root means square error (RMSE) from observation (CMAP) for **a**, **c** CAM4 and **b**, **d** CAM5. Units are in mm/day

found in the recent study by Meehl et al. (2012). Apart from the SAM region, the EAM system, covering both subtropics and mid-latitudes, is well captured in both models. CAM5 shows spatial patterns similar to those observed whereas the CAM4 simulation is drier than observations over the South China Sea. All simulations show very good correlation and RMSE skill for the EAM, compared with the SAM.

In the observed 850 mb wind pattern (Fig. 3c), the most important features are the monsoon westerlies, the northward movement of the low pressure area from the Bay of Bengal and the low level jet stream passing across the equator onto the Indian sub-continent. The strengthening of westerly 850 mb winds during the summer monsoon seasons can be seen in both models (Fig. 3a, b) over the 10°N–25°N latitude belt extending eastward from the western Arabian Sea through India and Bay of Bengal. The Bay of Bengal is considered as the moisture source of heavy precipitation events over the central South Asian region (Malik et al. 2010) and precipitation over this central region is mainly caused by the northward movement of low pressure areas from the Bay of Bengal (Lal et al. 1995). This interpretation is seen in both CAM4 and CAM5 simulations showing strong winds flowing from the Bay of Bengal to the north over central South Asia. In general, CAM4 and CAM5 are able to simulate the wind circulation at 850 mb (such as the equatorial monsoon flow and lower level jet stream) realistically, even though there are biases in the strength of monsoon westerlies over the Indian region.

The simulation of the seasonal migration of the ITCZ is a challenging issue in GCMs. Many studies (such as Hack et al. 1998 and Wu et al. 2003) reported that most GCMs are unable to reproduce the seasonal migration of the ITCZ

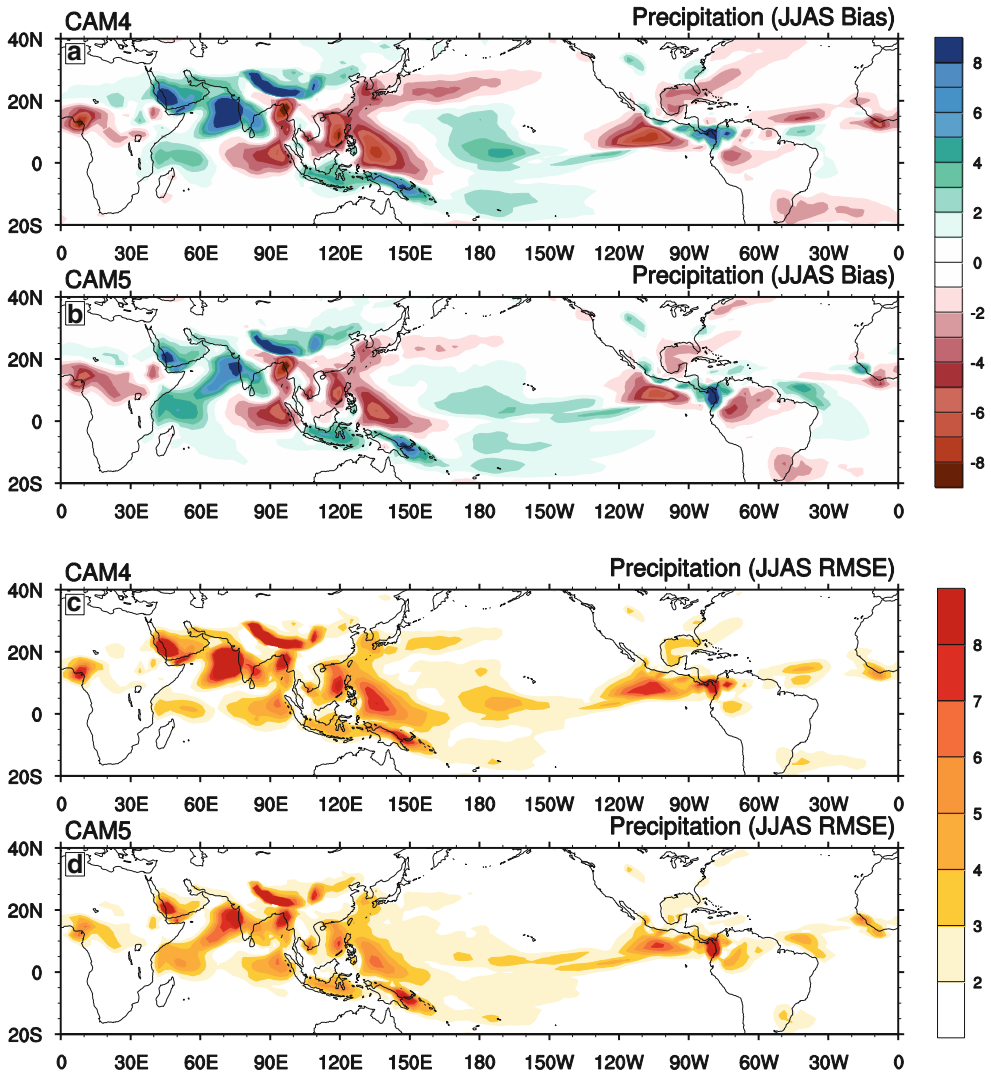

Fig. 2 Same as Fig. 1 but for the summer season (June–September; JJAS)

precipitation. Gadgil and Sajani (1998) found that the atmospheric models which can simulate the northward migration of the ITCZ can also simulate the interannual variation of the Indian monsoon reasonably well, whereas in models with poor SAM simulation, the ITCZ remains over the equatorial oceans in all seasons. Over the SAM region, the seasonal migration of the ITCZ from the equatorial region in winter to the heated continent in summer is the most important feature of the seasonal variation. We therefore briefly analyzed the seasonal migration of ITCZ in our model simulations by analyzing the mean January and July surface winds (not shown). It is found that this planetary scale feature of the general circulation is well captured by both CAM4 and CAM5. Also the location and strength of both the westerly jets over the northern Indian region during January and the tropical jets during July (early Monsoon) are fairly well reproduced in simulations which indicate that both models realistically capture the large shift of the ITCZ from January to July.

We have also performed simulations of CAM4 and CAM5 at higher resolution (0.9° × 1.25°) to analyze the effect of better resolved topography (which is an important aspect for the simulation of precipitation). We found (not shown here) that increasing the resolution improved the simulation over areas of complex terrain such as the Western Ghats and Himalayas in the SAM region. The Western Ghats capture much of the rain on the Arabian Sea-facing side, while the other side of these mountains (to the east in southeastern India) remains dry in the summer season. This is a localized effect and can only be seen in the higher resolution simulation. Also in the higher resolution run, heavy precipitation on the coastal mountain slopes of Myanmar, across the Bay of Bengal, is well simulated but with the same overestimation in the amount

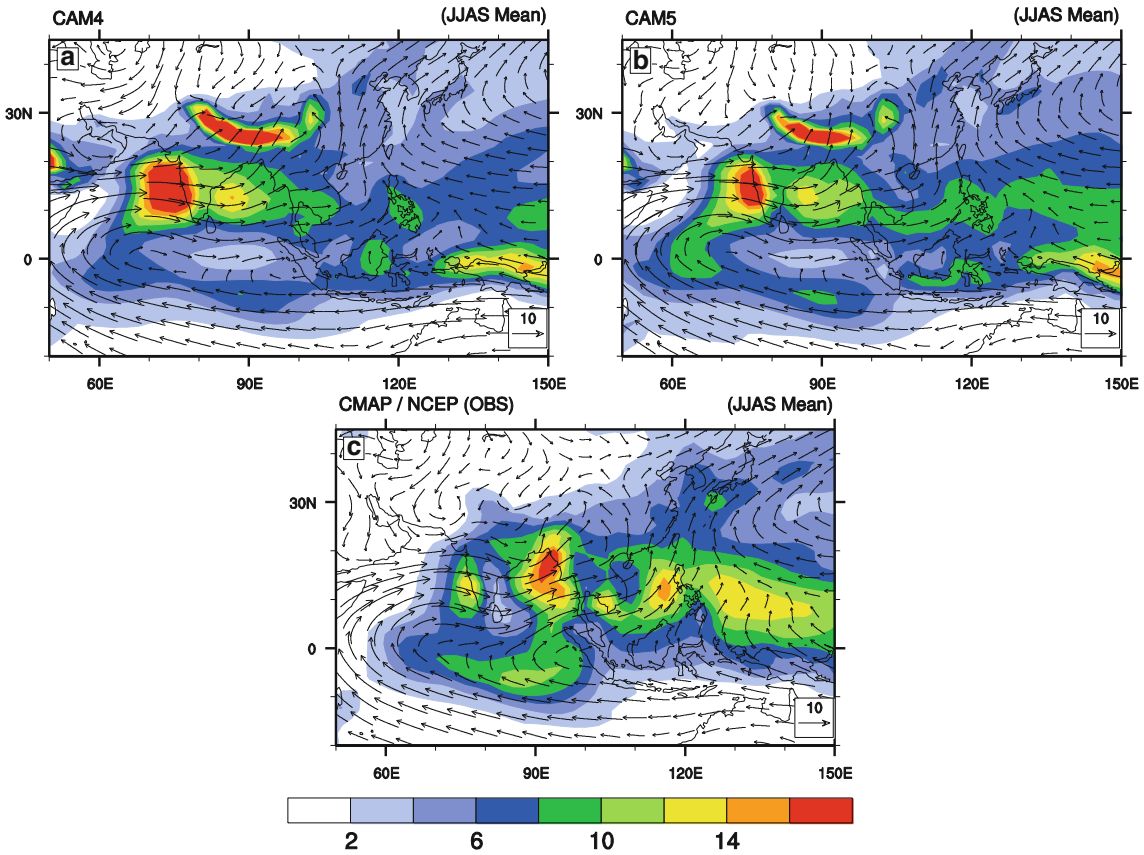

Fig. 3 Seasonal mean (June–September; JJAS) precipitation and 850 mb winds from: **a** CAM4, **b** CAM5 and **c** observations (CMAP/NCEP). Precipitation (*shaded*) in mm/day and 850 mb wind (vectors) in m/s

as seen in the lower resolution run. Also the excessive precipitation over the Tibetan Plateau in CAM4 (also the case in CAM5) is reduced in its higher resolution simulation. Both higher resolution simulations are somewhat closer to observations for the complex terrain regions of the SAM.

The seasonal evolution of SAM precipitation is examined in time-latitude diagrams averaged over the SAM longitudes (50°–120°E) for observations, CAM4 and CAM5 (Fig. 4). In the observations (Fig. 4c), a well-defined seasonal precipitation pattern that varies with latitude and moves significantly northward from 5°N in winter to 20°N in summer is visible. In models (Fig. 4a, b), the northward shift of precipitation starting in winter and reaching a maximum in summer is well captured but there are considerable systematic errors such as the simulated summer precipitation northward extent reaching too far north with a second maximum around 30°N. In the CAM4 and CAM5 simulations, the precipitation reaches a maximum at 15°N and exhibits an essentially realistic seasonal migration, but the simulations have heavier than observed precipitation over the Western Ghats. The overestimation is higher in CAM4 than in CAM5 along with more penetration of precipitation toward the north. In CAM5, the maximum contour of precipitation is somewhat reduced and is comparable to observations. The annual cycle of precipitation averaged over the latitude and longitude of the SAM region is simulated quite well in models, with a well-defined seasonal cycle as shown in Fig. 4d. Several characteristics of the annual cycle of SAM precipitation, such as the rapid onset between May and June, the sustained high precipitation from June to August and the slow withdrawal during September–October, are well simulated by both models. As noted earlier in the discussion of spatial patterns, both models produce realistic seasonal variation of precipitation in the SAM region, but with considerable overestimation. The annual cycle highlights this overestimation more clearly by showing excessive precipitation in the months July, August and September as well as in December, January and February.

From the above discussion of mean climatology simulations, it is seen that CAM5 has significantly improved simulations compared to CAM4. We further investigated this improvement by performing different sets of CAM5 simulations using the same radiation (CAMRT), aerosol (BAM) and boundary layer (HB, Holtslag–Boville 1993)

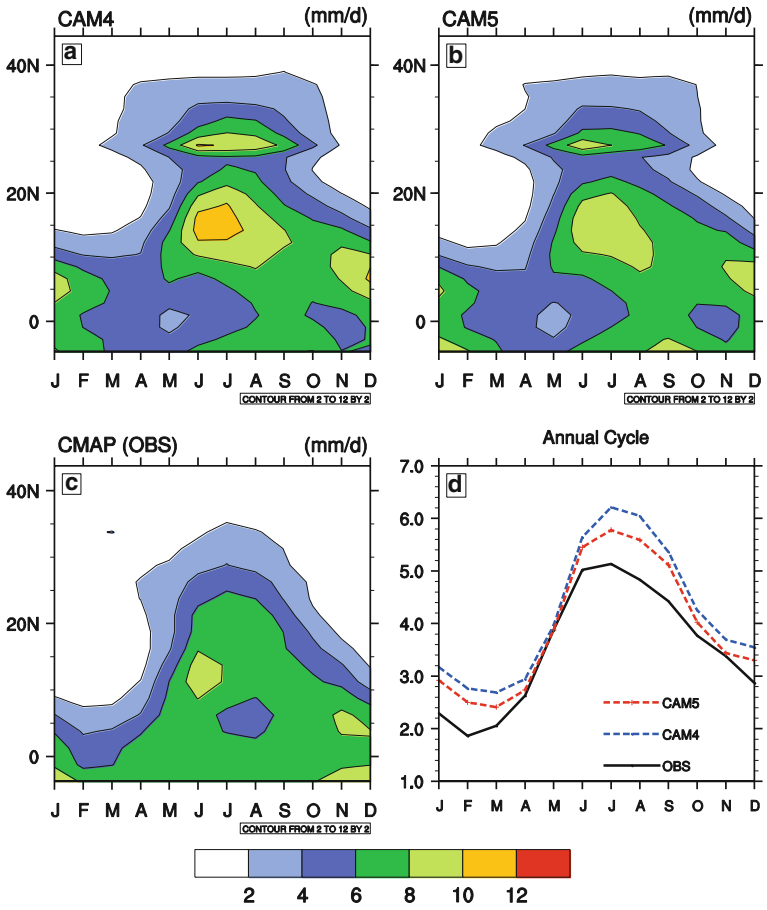

Fig. 4 Time-latitude evolution of precipitation averaged over (50°–120°E) for: **a** CAM4, **b** CAM5, **c** observations (CMAP) and **d** represents annual cycle of precipitation area averaged over SAM region. Units are in mm/day

schemes which are used in the CAM4 default configuration. This switching of new schemes (in CAM5) with old ones (in CAM4) allowed us to explore the effect of each individual scheme in improving CAM5 simulations over the SAM. We named each individual experiment of CAM5 as CAM5_BAM, CAM5_BAM_CAMRT, CAM5_BAM_HB and CAM5_BAM_CAMRT_HB (see Table 1 for details). Figure 5 represents the precipitation difference (JJAS) of CAM5_BAM, CAM5_BAM_CAMRT, CAM5_BAM_HB and CAM5_BAM_CAMRT_HB from observation. Comparing these differences, with the default CAM4 and CAM5 runs (Fig. 2a, b), reveals that the implementation of new boundary layer schemes (UW moist turbulence) in CAM5 has the greatest effect (in our case) on decreasing the overestimation seen in the CAM4 simulation. As reported by Park and Bretherton (2009), the new UW moist turbulence scheme improved the cloud top boundary layers in the CAM model. They used the CAM3.5 version to test this scheme and found significant reduction in model bias. In our case, although the new RRTMG radiation scheme and the full representation of aerosol indirect effects do not contribute as much to the improved SAM simulation, virtually every atmospheric process (revised/replaced) and its physical representation in the new version makes an improvement in the simulation (the individual discussion of all these new features of CAM5 is beyond the scope of this study).

3.2 Monsoon interannual variability

In this section, the monsoon variability is examined by focusing on the simulation of monsoon indices (precipitation and circulation) for both CAM4 and CAM5 models. The strong and weak monsoon composite analysis is also discussed to further explore the simulation's interannual variability. It has been well recognized that the interannual variability of many climatological variables on earth can stem from ENSO, which is the strongest interannual variability of the earth's climate system. Thus, the link between simulated SAM precipitation and ENSO is also explored using lag correlation. This is also performed to explore the relationship between the Indian Ocean Dipole (IOD, Saji et al. 1999) and SAM precipitation.

3.2.1 Asian monsoon indices

We examined the models simulations of monsoon interannual variability with several commonly used monsoon

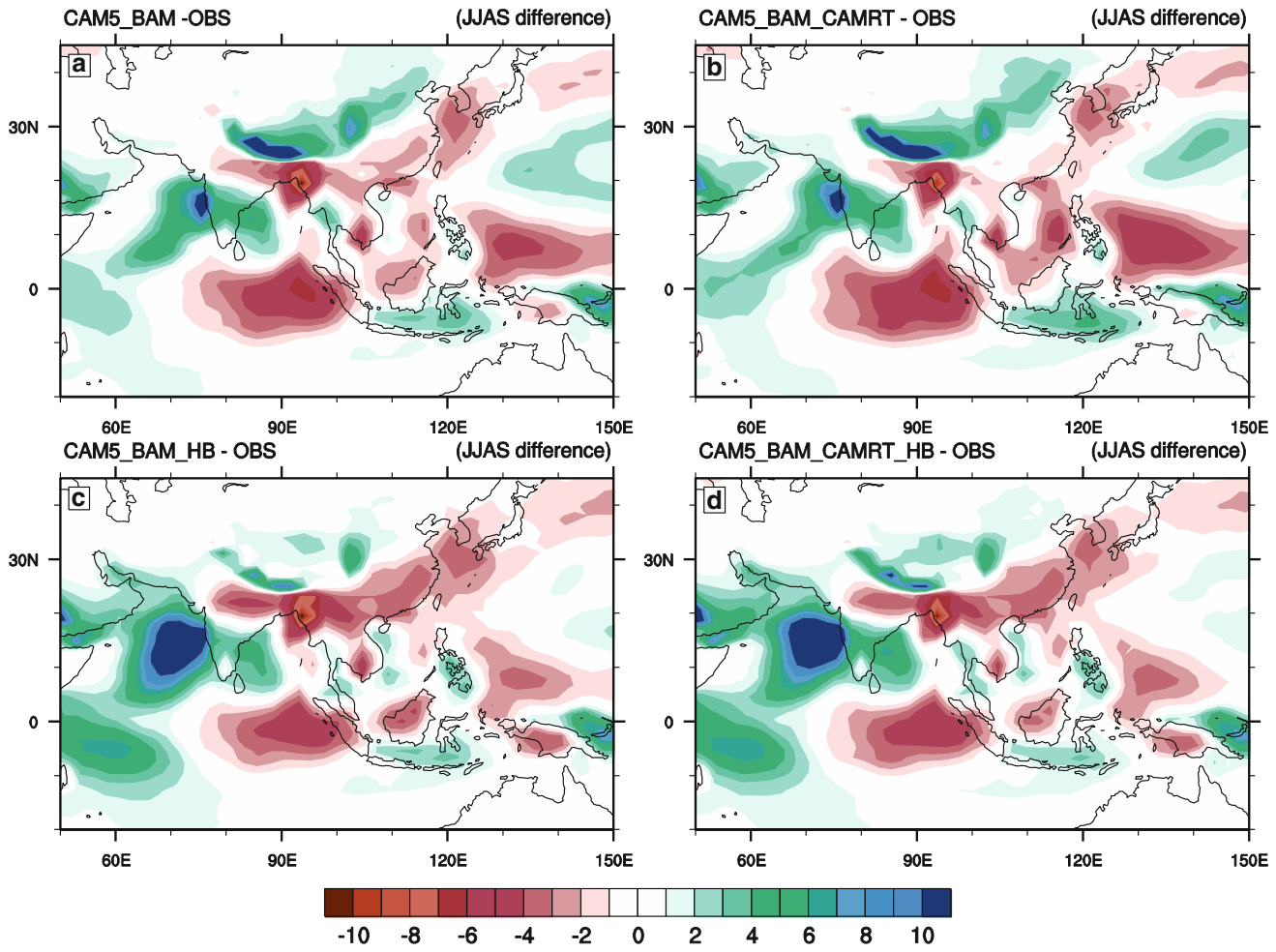

Fig. 5 Seasonal mean (June–September; JJAS) precipitation differences from observations (CMAP) for: **a** CAM5_BAM (CAM5 with bulk aerosol model (BAM) scheme), **b** CAM5_BAM_CAMRT (CAM5 with BAM and CAMRT (radiation) schemes), **c** CAM5_BAM_HB (CAM5 with BAM and HB (Holtslag–Boville, boundary layer turbulence) schemes) and **d** CAM5_BAM_CAMRT_HB (CAM5 with BAM, HB and CAMRT schemes). Units are in mm/day

indices, including Indian Summer Rainfall (ISR), the Webster–Yang monsoon index (WY index) (Webster and Yang 1992), the Southeast Asian monsoon (SEAM) index or Western North Pacific monsoon (WNPM) index (Wang and Fan 1999), Indian monsoon (IM) index (Wang et al. 2001) and South Asian monsoon index (SAM_i, here the subscript i denotes "index" to differentiate it from SAM) (Goswami et al. 1999). The definitions of these indices are given in Table 2.

Figures 6 and 7 show the simulated and observed interannual variability of ISR, WY, IMI, WNPM, and SAM_i monsoon indices normalized with their respective standard deviation. All these indices are circulation indices except ISR which represents SAM precipitation. To analyze model simulations for individual strong and weak monsoons, the ISR index is separated from the circulation indices (Fig. 7) and is presented in Fig. 6. In Fig. 6a, the observed ISR index representing the strength (strong and weak monsoon) and interannual variation of SAM precipitation, is shown. Strong monsoon years such as 1980, 1988 and 2007 are differentiable in the observations, whereas in CAM4 and CAM5 (Fig. 6b, c) only the year 1988 has the same sign. Both 1980 and 2007 are characterized as weak monsoon years in both models—opposite to the observations. Similarly, the observed weak monsoon years 1984, 1986 and 2002 are simulated as strong monsoon years in model. This means that both CAM4 and CAM5 failed to capture the interannual variability of the SAM, except in some years. We find that there are large errors in the simulation of some extreme seasons which leads to the overall poor skill. Considering SAM extreme precipitation, for those associated with ENSO, both models simulate at least the sign of SAM accurately. For example, the La Nina of year 1988 was successfully simulated by both models while CAM4 failed to spatially capture the El Nino year of 1987. This analysis suggests that the low skill in simulation

Table 2 Details concerning frequently used Asian monsoon indices

Name of the index	Type of index	Definition	References	Correlation	
				CAM4	CAM5
Indian summer rainfall (ISR)	Precipitation	PREC (5°–40°N, 60°–100°E) Averaged JJAS precipitation over the domain	–	−0.13	−0.31
Webster–Yang monsoon (WY)	Circulation	U850–U200 (0°–20°N, 40°–110°E) Vertical shear of zonal winds between 850 and 200 mb levels	Webster and Yang (1992)	0.38	0.45
Western North Pacific monsoon (WNPM)	Circulation	U850 (5°–15°N, 90°–130°E) − U850 (22.5°–32.5°N, 110°–140°E) Difference of 850 mb zonal winds	Wang and Fan (1999)	0.66	0.60
Indian monsoon (IM)	Circulation	U850 (5°–15°N, 40°–80°E) − U850 (20°–30°N, 70°–90°E) Difference of 850 mb zonal winds	Wang et al. (2001)	−0.037	−0.11
South Asian monsoon index (SAM_i)	Circulation	V850 − V200 (10°–30°N, 70°–110°E) Vertical shear of meridonal winds between 850 and 200 mb levels	Goswami et al. (1999)	−0.26	−0.13

The last two columns give the correlation of simulated indices with observations for both CAM4 and CAM5

of monsoon interannual variation arises mainly from a poor simulation ENSO–monsoon teleconnections rather than the lack of air–sea interaction (coupling). Since the SAM has remote and local SST teleconnections, the poor simulation of SAM interannual variability in these atmospheric models (forced with observed SST) can be explain by analyzing the ENSO–monsoon teleconnection and regression of Nino SST on SAM precipitation. We will further discuss this issue in the next section.

In case of circulation indices (Fig. 7), it is seen that both CAM4 and CAM5 show considerable skill in simulating the interannual variation of the WY and WNPM indices with significant correlation coefficients (see Table 2). For the IM and SAMi indices, correlation coefficients are insignificant, meaning that these indices are not well simulated in these models. As the WNPM index represents the East Asian summer monsoon, the significant higher correlation of this index means that East Asian monsoon circulations are better simulated in both models compared to the SAM. Analyses of monsoon spatial patterns also support this result. This may be due to the fact that the East Asian monsoon has a stronger response to ENSO than the Indian monsoon.

To get better insight into the simulated circulation in CAM4 and CAM5 simulations, JJAS mean velocity potential and divergent wind anomalies are calculated for both models and observations (NCEP). These show upper-level convergence and lower-level divergence over the equatorial central Pacific, and upper-level divergence and lower-level convergence over the SAM region (not shown here). In Fig. 8, we analyze the difference between model and observation (NCEP) of the JJAS mean velocity potential and corresponding divergent winds at 850 mb and 200 mb. Although some of the circulation indices have higher correlation for CAM4 than CAM5, the overall spatial patterns from the CAM5 simulations are better. At both atmospheric levels, over the Pacific and Indian regions, CAM5 have much better skill (less difference) compared to CAM4.

3.2.2 *Composite analysis*

Modeling extreme events is one of the most challenging issues and validating model extreme event simulations is therefore important to assess their performance. In this subsection, we will focus on several particular years which were recorded as strong and weak monsoon years over SAM region (as seen in Fig. 6). Strong and weak monsoon years are characterized on the basis of significant weak or strong summer precipitation over the monsoon region. Years with anomalies of summer mean precipitation greater than 0.5 standard deviation above the mean are categorized as strong monsoon years (1980, 1981, 1983, 1988, 1994, 1996, 1998 and 2007) and those with mean precipitation less than −0.5 standard deviation below the mean are categorized as weak monsoons (1982, 1984, 1986, 1987, 1989 and 2002). Composites of strong and weak monsoon years from observations (CMAP), CAM4 and CAM5 are shown in Fig. 9. The observed strong and weak monsoon composites have a large-scale structure with anomalies of the same sign over many parts within the SAM region (Fig. 9a, b). The observed weak monsoon composite has negative anomalies over the whole Indian region whereas in the strong monsoon composite there are positive anomalies over the Indian land area, Bay of Bengal, and the maritime continent, while there are

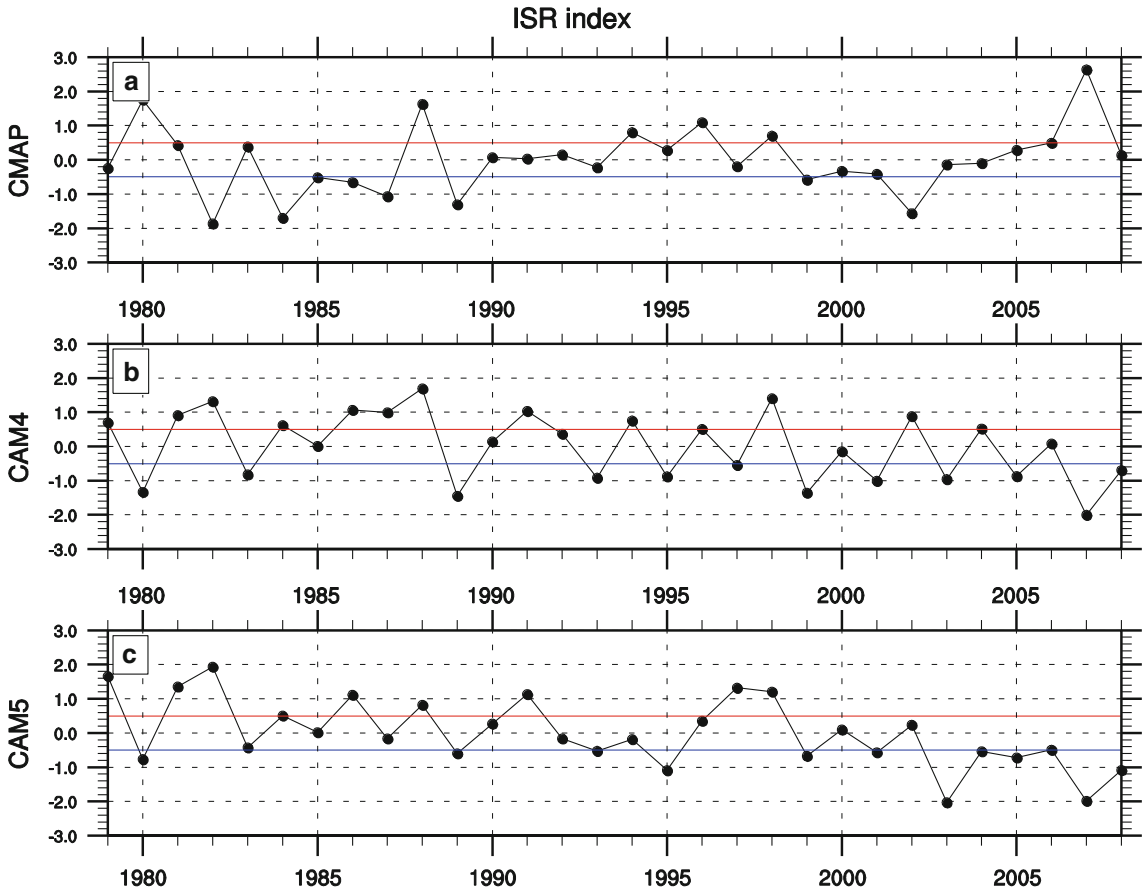

Fig. 6 Time series of Indian summer rainfall (ISR) index for **a** CMAP, **b** CAM4 and **c** CAM5. Details of this index are given in Table 1. The time series are normalized and thus unitless

negative anomalies over the equatorial Indian Ocean. The increased precipitation during a strong monsoon over the Indian monsoon region is accompanied by a decrease in precipitation over the equatorial eastern Indian Ocean. The models composites (Fig. 9c–f) show that the simulations failed to reproduce the observed anomaly patterns with some areas having significant differences. For its weak monsoon composite, CAM4 and CAM5 have a much different pattern with more intense and large scale positive anomalies (which is opposite from the observed composite patterns) over the Western Ghats and Bay of Bengal. CAM4 and CAM5 to some extent, reproduce the strong monsoon composite over southern India. In short, both models show poor skill in differentiating the strong and weak monsoon years. This is also seen in the models ISR index (Fig. 6) as both showed poor skill in simulating the interannual variability of the SAM region. This is probably due to the simulated overestimation of precipitation, as well as strong internal dynamics (noise) in the models. An examination of the interannual variability of CAM4 and CAM5 monsoon simulations showed that, although the observed SST tends to enhance the variability, the internal dynamics also produce considerable interannual variability in these simulations. It is interesting to note that the large variance in control runs is dominated by a few events such as 1983, 1988 and 2007. For many years, the interannual variability produced by internal dynamics is often larger than that in the control runs, suggesting that the interannual variability generated purely by internal dynamics is comparable to that forced by the slowly varying SST boundary forcing in many cases. This is probably the reason why these models perform poorly in differentiating strong and weak monsoon seasons.

3.3 Teleconnection of SAM with ENSO and IOD in CAM simulations

In this section, we explore how well CAM4 and CAM5 capture SAM–ENSO and SAM–IOD relationships. We perform regression analysis to analyze spatial patterns of these relationships whereas lag-lead correlation is used for temporal analysis. Figure 10 shows the linear regression of Nino3.4 (−5°S–5°N, 120°–170°W) and IOD [(−10°S–10°N, 50°–70°E) − (−10°S–0°, 90°–110°E)] SST indices

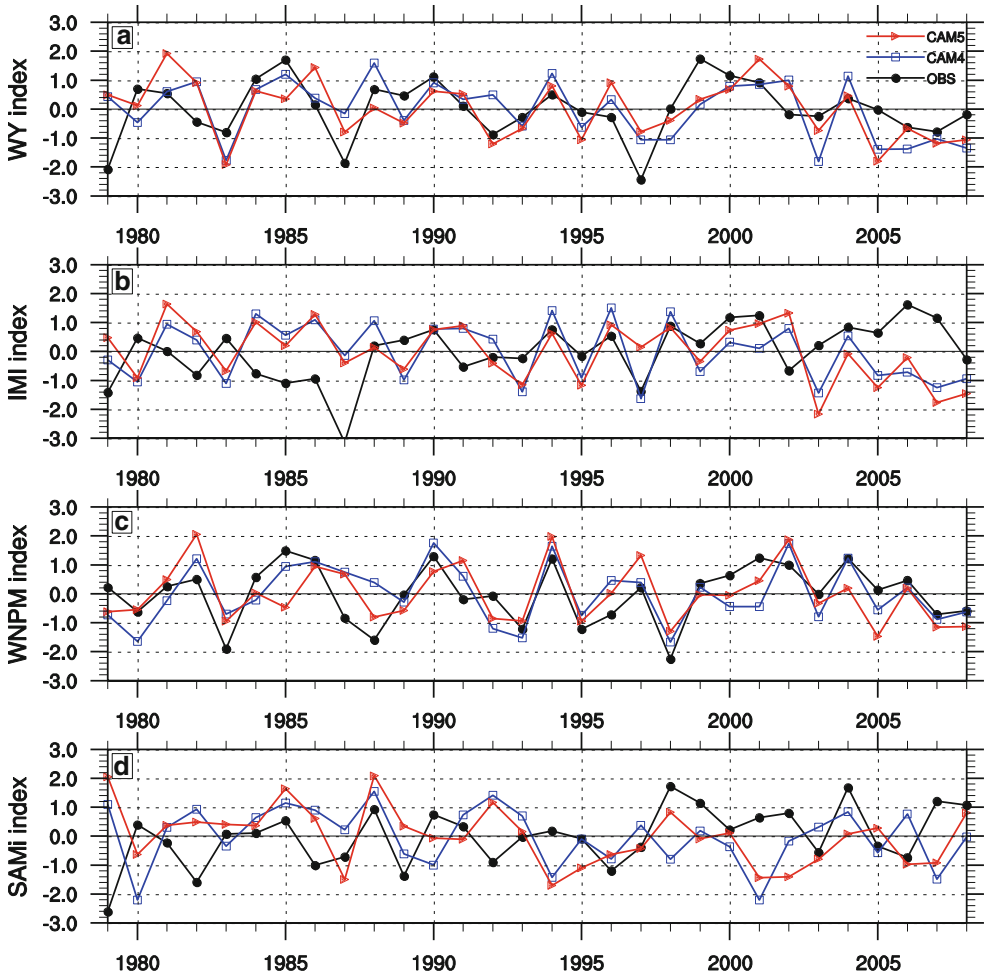

Fig. 7 Time series of **a** Webster–Yang (WY) index, **b** Indian monsoon index (IMI), **c** Western North Pacific monsoon (WNPM) index, and **d** South Asian monsoon (SAM_i) index of observation (CMAP/NCEP, *black line*), CAM4 (*blue line*) and CAM5 (*red line*). Details of all the indices are given in Table 1. The time series are normalized and thus unitless

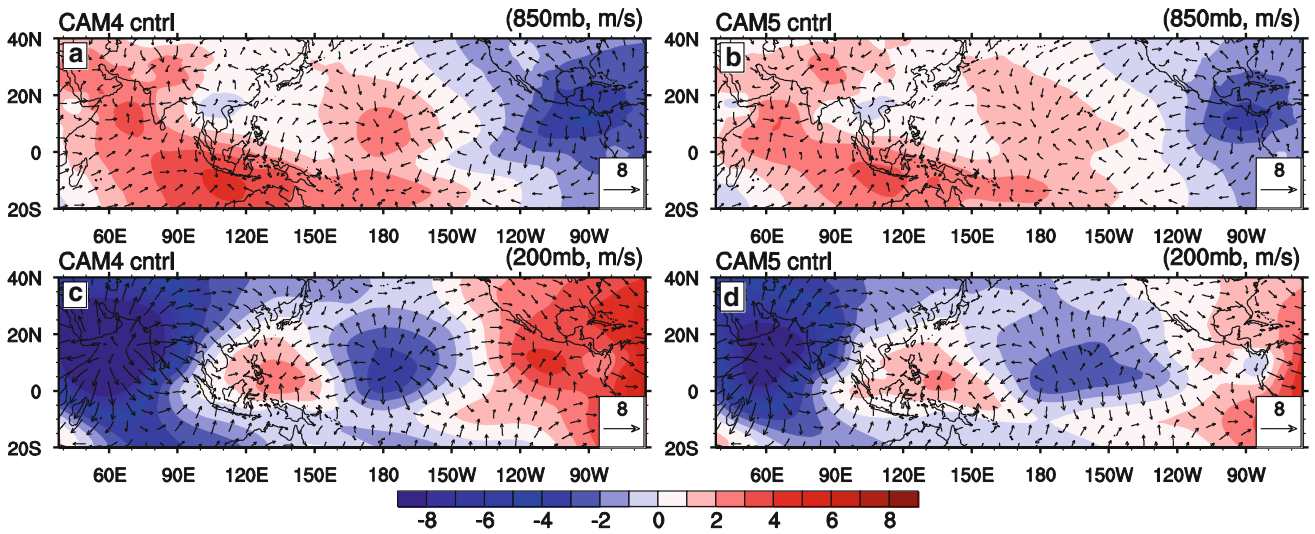

Fig. 8 Difference between model (CAM4 and CAM5) and observed (NCEP) JJAS mean velocity potential (10^{-6}/s) and corresponding divergent winds (m/s) at **a**, **b** 850 mb and **c**, **d** 200 mb

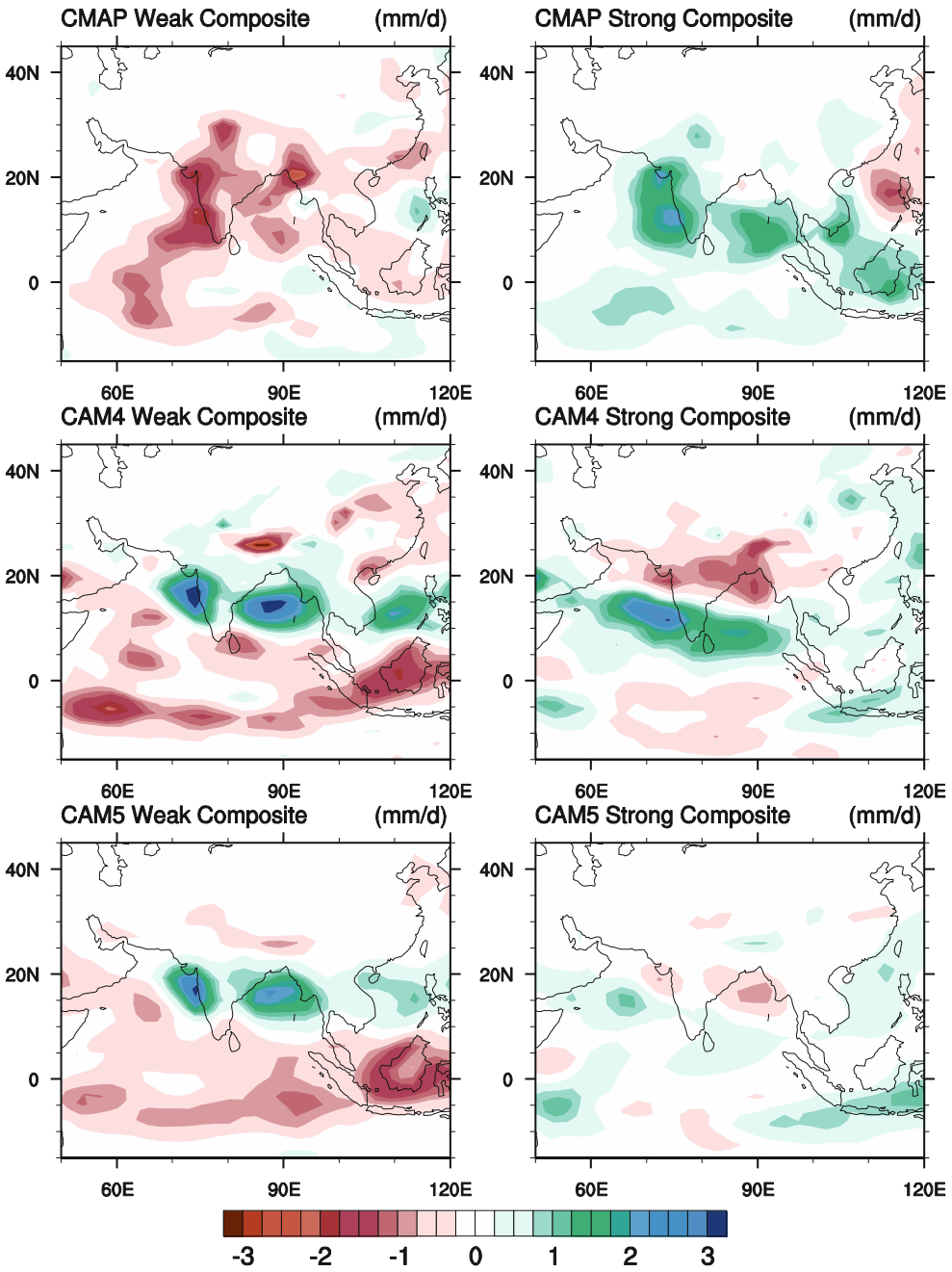

Fig. 9 June–September (JJAS) anomaly precipitation composites of weak (1982, 1984, 1986, 1987, 1989 and 2002) and strong (1980, 1981, 1983, 1988, 1994, 1996, 1998 and 2007) monsoon years for **a**, **b** observation (CMAP), **c**, **d** CAM4 and **e**, **f** CAM5. Units are in mm/day

with JJAS precipitation and 850 mb winds for observations and both models. Unless stated otherwise, all regression maps show the covariance of the normalized Nino3.4 and IOD indices. The regression of precipitation and 850 mb wind onto the Nino3.4 index is an important key to understanding the behavior of CAM4 and CAM5 in simulating realistic ENSO properties as these fields are direct indicators of the connection between the ocean and the atmosphere. In Fig. 10a, the regression of the observed Nino3.4 index with precipitation and 850 mb winds is shown. The observations reveal enhanced precipitation over the Bay of Bengal, accompanied by a westerly wind anomaly and decreased precipitation over most of the Indian region. In the models' results (Fig. 10c, e) quite realistic patterns are seen over the equatorial Indian Ocean whereas over the Western Ghats and central India, both CAM4 and CAM5 have opposite response compared to observations. In the IOD regression pattern (Fig. 10d, f), spatial modes are well reproduced over the Indian Ocean (enhanced precipitation over the Western equatorial Indian

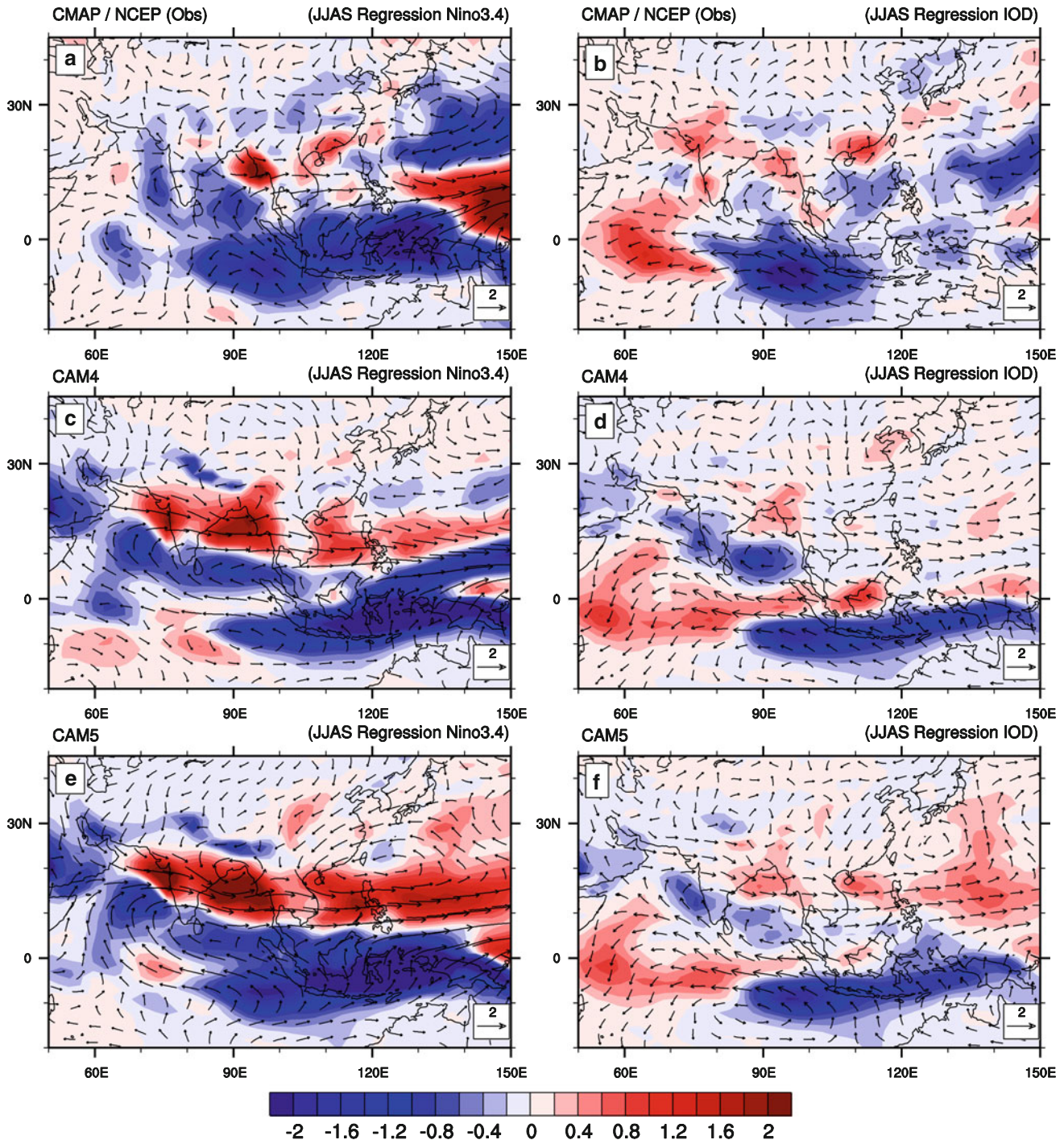

Fig. 10 The linear regression of observed June–September (JJAS) Nino3.4 (−5°S–5°N, 120°–170°W) and IOD [(−10°S–10°N, 50°–70°E) − (−10°S–0°, 90°–110°E)] SST indices with June–September (JJAS) observed and simulated precipitation and 850 mb winds. **a**, **b** Observation (CMAP/NCEP), **c**, **d** CAM4 and **e**, **f** CAM5

Ocean and decreased precipitation over the Eastern Indian Ocean) whereas over the Indian continent the models have the opposite sign similar to the ENSO regression.

The analysis above showed that precipitation response to local and remote SST in the models' simulations is not preserved. To further investigate this issue, the lagged correlation of Nino3.4 and IOD indices with the simulated ISR index is shown in Fig. 11. The area averaged (0°–40°N, 55°–100°E) time series of observed CMAP precipitation (ISR, solid black line), observed All-India Precipitation (AIR) index (dashed black line) and simulated (CAM4, solid blue line and CAM5, solid red line) time

series are correlated with observed Nino3.4 and IOD SST indices. The months with negative (positive) sign indicate that SST leads (lags) the ISR with maximum lead of 12 months (1 year). Months 0 and 12 indicate June whereas months 4 and 8 correspond to February and October (minus sign for previous months). Correlations are calculated using a 5 month sliding window. The observed positive correlations occur when the SST leads the SAM precipitation and negative correlations occur when SST lags the SAM precipitation. A negative correlation is seen for SST from the same summer to the following winter, showing a weak (strong) SAM in El Nino (La Nina) developing years. The highest negative correlations are noted if the monsoon lags Nino 3.4 SSTs which suggests, as reported in Kirtman and Shukla (2000), that monsoons can provide favorable conditions for triggering or enhancing El Nino or La Nina events in the Pacific during the following winter. The observed ISR index has significant lagged and lead correlations with SST, with the highest value of around 0.5 when monsoon precipitation is slightly led by SST. This suggests a cross-interaction between monsoon and ENSO, namely, ENSO impacts on SAM precipitation and meanwhile the monsoon variability may affect the ENSO evolution, intensity, and periodicity. The mutual influence between ENSO and SAM has been widely reported in other studies as well (Chung and Nigam 1999; Kitoh and Arakawa 1999; Meehl and Arblaster 1998; Wang et al. 2004). It is noted that the difference in correlation magnitude between Fig. 11a and those in other studies (Kirtman and Shukla 2000; Yasunari 1990) may be accounted for by a dramatic change of the ENSO–SAM relationship in the late 1970s, since Fig. 11a is obtained only using the data after 1979. In the CAM4 and CAM5 simulations, this relationship is poorly captured, particularly when SST lags monsoon. CAM4 shows a somewhat comparable result when SST leads monsoon. Both of these models failed to maintain the monsoon and ENSO relationship because, as discussed in the composite analysis, the internal dynamics of these models can overwhelm the Pacific SST influence on monsoon precipitation. In Fig. 11b, the lag-lead correlation of SAM with IOD is computed. A positive correlation during late spring and the simultaneous summer is seen. The correlation changes to negative in the following fall, suggesting a negative feedback of SAM on the IO. For the models, the simultaneous response is not clear but when IOD leads monsoon, both models show a comparable response to observation.

Overall the above analysis shows that the interannual skill of CAM4 and CAM5 in simulating SAM is poor. Both models failed to differentiate strong and weak monsoon which is indirectly linked to their poor reproduction of the ENSO–monsoon relationship. The correct representation of the ENSO–SAM relationship in models is crucial, since it is the basis for seasonal forecasts of SAM using climate models. The poor skill of CAM4/CAM5 interannual variability, even when forced by observed SST, is attributed to the models' poor skill in simulating the SST–precipitation relationship over the Indian and Pacific oceans and a lack of atmosphere–ocean coupling that has been reported as critical for skillful simulation of the monsoon (Wang et al. 2005). Since this lack of atmosphere–ocean coupling in GCMs is one of the possibilities for their poor skill, we focus our analysis on the coupled CCSM4 model in the next section and will compare its simulation with CAM4 and observations.

4 Coupled simulation using CCSM4

We now investigate the mean climatology and relationship between SAM precipitation and SST in the CCSM4 fully coupled model, which will allow insight into the role of coupling on the simulation of SAM precipitation. As previously discussed, CCSM4 uses CAM4 as its atmospheric model and POP2.2 as its ocean model. Along with observations, we will also contrast CCSM4 with the CAM4 results presented in previous sections. Here we will mainly use the CCSM4 climatology run whereas for some sensitivity experiments, data from a CCSM4 transient run (CCSM4_TR, downloaded from NCAR) forced with observed forcing of green house gases) is also used.

4.1 Mean climatology of CCSM4

We first analyze, as for the atmospheric simulations, the coupled model over the tropical region including both Indian and Pacific Oceans. Figure 12b shows the observed (CMAP) JJAS mean precipitation differences (in mm/day). The difference between the CAM4 climatology run (CAM4_CLIM) and observations is also shown in Fig. 12a. CCSM4 shows significant differences, particularly over the Indian and Pacific Ocean. Specifically, the coupled simulation underestimates precipitation over the western and eastern equatorial Pacific and over the eastern Indian Ocean, and it overestimates precipitation over the western Indian Ocean and central equatorial Pacific Ocean. These differences, shown in Fig. 12, result from the ocean component of CCSM4. The SST bias from the ocean model influences the precipitation directly, making it different from the observed precipitation climatology. Comparing CCSM4 with CAM4_CLIM shows that CCSM4 precipitation biases are at a broad scale (especially over oceans). In CCSM4, the negative precipitation bias increases over the equatorial area in the Pacific Ocean. This is probably due to the feedbacks of ocean-air coupling in the coupled model that amplifies the bias in the atmospheric and

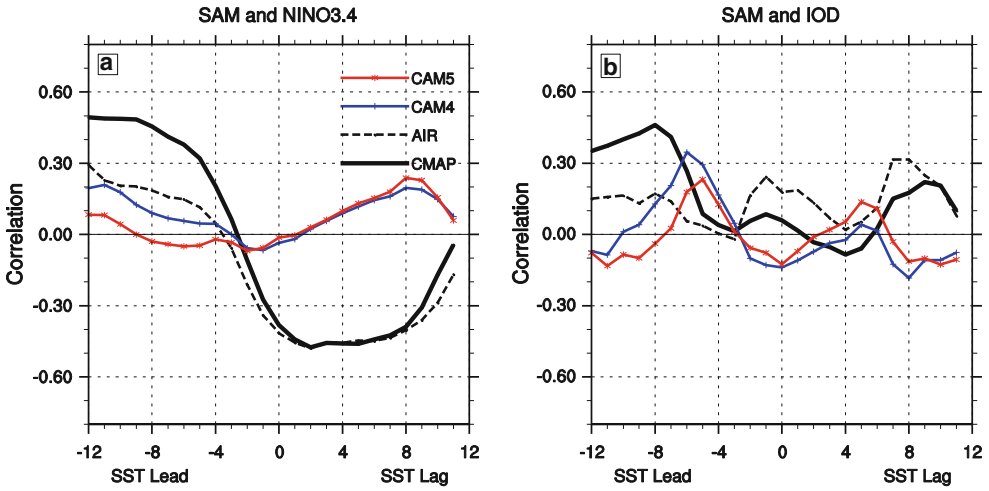

Fig. 11 Lag-lead correlation of monthly mean precipitation with **a** Nino3.4 (−5°S–5°N, 120°–170°W) and **b** IOD [(−10°S–10°N, 50°–70°E) − (−10°S–0°, 90°–110°E)] indices. Area averaged (0°–40°N, 55°–100°E) time series (ISR) of observed CMAP (*solid black line*) precipitation, observed All-India Precipitation (AIR—*dashed black line*) time series and simulated (CAM4 *solid blue line* and CAM5 *solid red line*) time series are correlated with observed Nino3.4 and IOD SST indices. The month with negative (positive) sign indicate that SST leads (lags) the ISR with maximum lead of 12 months (1 year). Month 0 and 12 indicates June whereas month 4 and 8 correspond to February and October (minus sign for previous month). Correlations are calculated using a 5 month sliding window

oceanic components. CCSM4 has the double ITCZ bias, characterized by heavy simulated precipitation over much of the tropical Pacific (central Pacific near 5° south) and the equatorial Indian Ocean, and light precipitation in the west and central Pacific between 15° and 30° south. The double ITCZ problem was also present in previous versions of the CCSM model. Lin (2007) found that most of the current coupled models and uncoupled models have this double ITCZ problem to some extent. Focusing on the SAM region reveals that while the CAM4 simulation overestimates precipitation over much of this region, the coupled simulation is more realistic and comparable to observations although the amounts are still overestimated somewhat. This is similar to results from the CCSM3 model reported in Meehl et al. (2006). The CCSM4 simulation has reduced bias over the Arabian Peninsula and the western coast of India (Fig. 12b), which is a direct consequence of the thermodynamic air–sea interactions in the Arabian Sea, Bay of Bengal, and South China Sea, which are absent in uncoupled simulations. Meehl et al. (2012) also reported that the CCSM4 simulation over the SAM region is much better than the CAM4 simulation. It is also reported in Wang et al. (2004) that the implementation of air–sea coupling could improve the model simulation of monsoon precipitation and circulation in the Asian monsoon. The absence of air–sea coupling in CAM4 results in continuous heating of the atmosphere by the prescribed SST (thus keeping the SST warm) which increases the evaporation, resulting in increased precipitation in those models. This positive feedback on precipitation amplifies the SAM variability and therefore CAM4 simulations overestimate precipitation in the SAM region. We will further discuss air–sea coupling and role of SST bias in the next section. In general, CCSM4 shows a large reduction in precipitation and less bias over the SAM region including the Arabian Sea, Bay of Bengal and equatorial Indian Ocean as compared with the CAM4 simulation. The reduction of SAM precipitation in the coupled model can also be seen in the seasonal cycle (not shown) averaged over the region.

Seasonal mean JJAS precipitation and 850mb wind from CCSM4 shown in Fig. 13 is more reliable and comparable to the observations than results from CAM4 and CAM5 (compare with Fig. 3). The extreme high precipitation area over the Northern West Indian Ocean is diminished in the coupled simulation making it more comparable to observations. However, CCSM4 also removed the heavy observed precipitation over the Bay of Bengal making its simulation different than observation. This is a significant shortcoming of the coupled simulation. Also, in CCSM4 runs, the precipitation is more concentrated in the western Indian Ocean, which was also seen in CCSM3 (Meehl et al. 2006). Considering these spatial patterns only, the overall mean climatology of CCSM4 seems to be more realistic and much better than from the uncoupled simulation, providing evidence that coupled air–sea interaction is necessary for climate models.

4.2 Teleconnection of SAM with ENSO in coupled simulation

A correct ENSO–monsoon relationship is one of the prerequisites needed for a coupled model to produce reliable

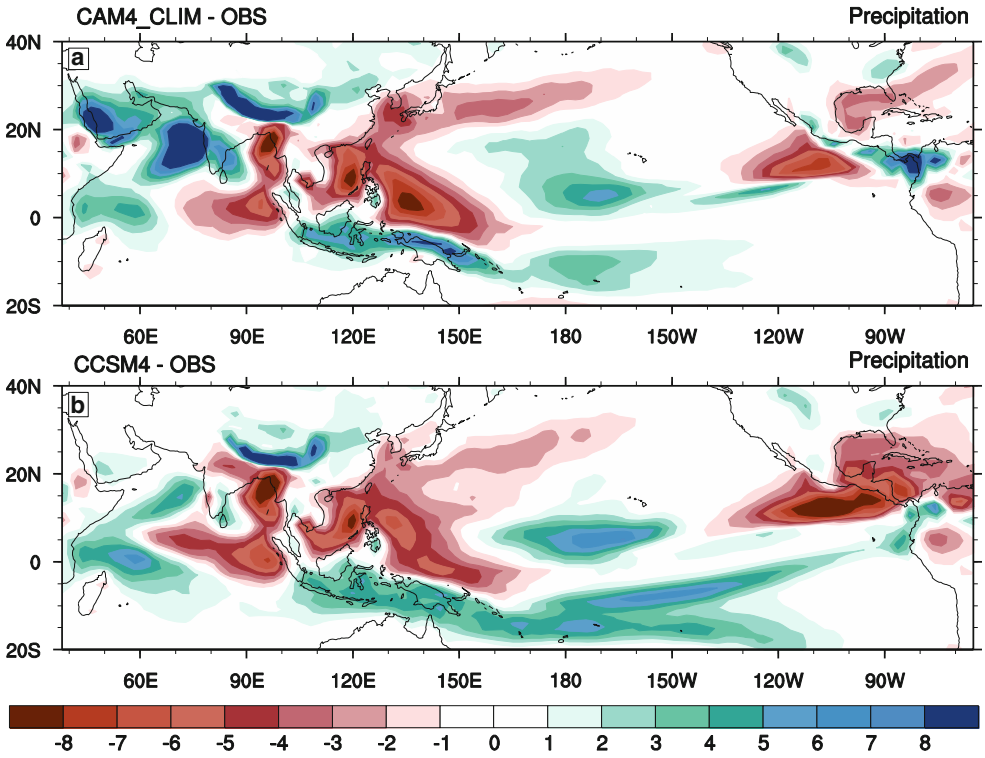

Fig. 12 June–September (JJAS) mean differences between simulation and climatology (CMAP) for: **a** CAM_CLIM (CAM4 climatology run) and **b** CCSM4. *Shading* corresponds to the precipitation difference in mm/day

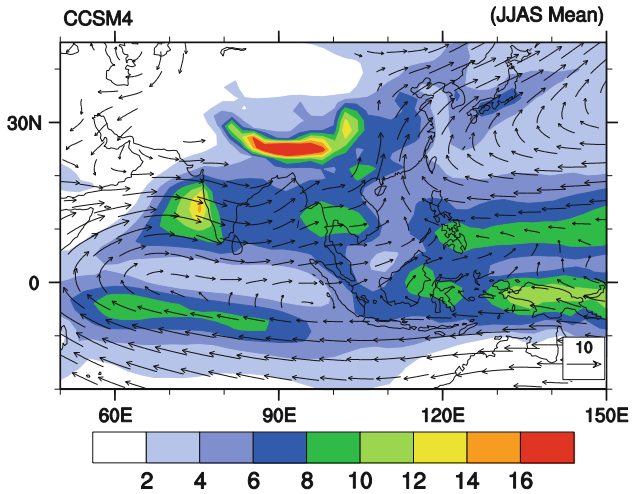

Fig. 13 Same as Fig. 3 but for CCSM4. Precipitation (*shaded*) in mm/day and 850 mb wind (vectors) in m/s

simulations of the monsoon. Here we document the ability of CCSM4 to reproduce the observed lead-lag relationships between the SAM and ENSO, and to understand how systematic errors may affect the simulation of this relationship. We first discuss the simulation of Nino3.4 and IOD indices in the coupled model. Figure 14 shows the variance spectrums of monthly Nino3.4 and IOD index for (a) observation and (b) CCSM4. In the observations, the broad peak shows a probable frequency of ENSO events of 3–6 years (0.24/year) with the maximum variance of about 20. In the CCSM4 simulation, the same frequency of 3–6 years is seen with maximum peak at 4 years although the CCSM4 Nino3.4 variability is significantly larger than the observed variability. In the previous version of CCSM i.e. CCSM3 the ENSO frequency (about 2 years) was reported as very poor by Collins et al. (2006a, b). This shows that new version of CCSM has significant improvements in its dynamics and can therefore simulate the ENSO properties more closely to observation. For the case of the IOD spectrum, being irregular in its oscillatory period, there is no well-defined peak in the observed frequency whereas in CCSM4, the peak of the IOD spectrum remains in phase with that of the Nino3.4 index showing a frequency of 3–6 years. Also these results show that the IOD index varies significantly with ENSO in CCSM4. The observed IOD variance is very small whereas the model variability is significantly larger showing a similar pattern as the Nino3.4 index.

Figure 15 (top) shows the linear regression of the CCSM4 simulated JJAS Nino3.4 (−5°S–5°N, 120°–170°W) SST index with JJAS precipitation and 850 mb winds. Comparison of this regression pattern with Fig. 10 reveals the improved spatial Nino3.4 regression pattern of the CCSM4 simulation, which is due to the improved and

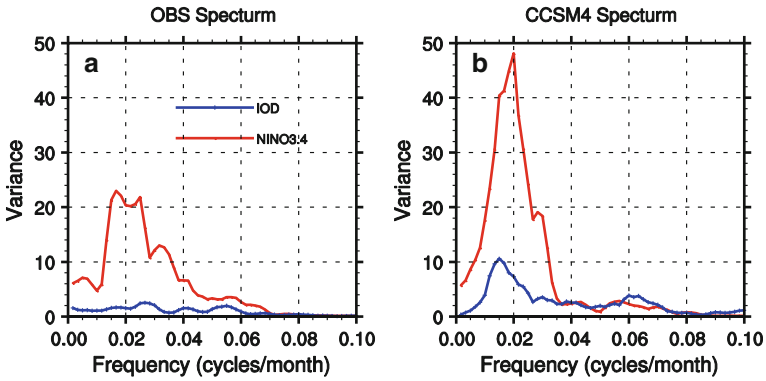

Fig. 14 The variance power spectrum for **a** observed SST (HadSST) and **b** CCSM4. Nino3.4 (−5°–5°N, 120°–170°W) SST index is in a *solid black line* and IOD [(−10°S–10°N, 50°–70E°) − (−10°S–0°, 90°–110°E)] index is in a *solid blue line*

coherent atmospheric response in coupling. This can be also seen in Fig. 15 (bottom), representing lag-lead correlation of CCSM4 simulated SAM precipitation with simulated Nino3.4 SST index. The observations show positive correlation when precipitation lags ENSO and strong negative correlations when precipitation leads ENSO. The CCSM4 can partially capture the observed variation of correlation timing but with quite different magnitudes. Comparing CCSM4 lag-lead correlation with CAM4 (Fig. 11) shows significant improvement in the coupled simulation relationship. This is probably due to an improved or consistent SST simulation and its interaction with atmosphere, which is absent in atmosphere-only simulations. The response of ENSO to SAM precipitation (i.e., SST lagging the monsoon) is realistic in CCSM4, better than in CAM4. The lag-lead correlation for ENSO suggests that in the CCSM4, SST has significant biases over the central equatorial Pacific and Indian Ocean. The fact that CCSM4 reveals a better connection between ocean and atmosphere in its simulation, although the Nino3.4 amplitude is considerably larger than the observed one, supports the low sensitivity to SST in the CAM4 model. Apparently, the atmospheric component i.e. CAM4 in CCSM4 shows a realistic response to ENSO variability only when being forced by a strong SST signal which is confirmed by CAM4 sensitivity experiments (not shown or discussed further here).

Since SST and precipitation are strongly coupled in the tropics, an unrealistic simulation of SST distribution should lead to an unrealistic SAM–ENSO relationship. To assess this we analyzed the average mean seasonal SST differences between CCSM4 and the observed climatology over the Indian and Pacific oceans. This also helps further investigate the SAM improvements in coupled simulations. In the observed mean SST climatology (not shown here) the most important feature is the warm pool region over the west Pacific with SSTs more than 28.0 °C and a cold SST tongue along the east Pacific associated with easterly trade winds along with a strong east–west SST gradient across the equatorial Pacific. A north–south irregularity is present

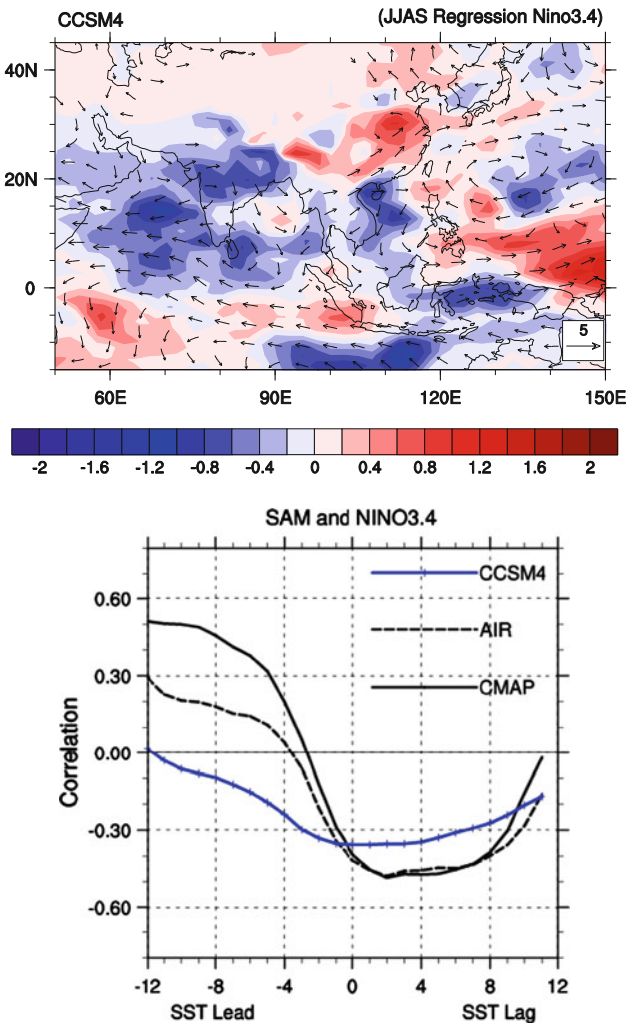

Fig. 15 The linear regression (*top*) of CCSM4 June–September (JJAS). Nino3.4 (−5°S–5°N, 120°–170°W) SST index with June–September (JJAS) simulated precipitation and 850 mb winds. Lag-lead correlation (*bottom*) of CCSM4 monthly mean precipitation with CCSM4 Nino3.4 (−5°S–5°N, 120°–170°W) SST index. Area averaged (0°–40°N, 55°–100°E) time series (ISR) of observed CMAP (*solid black line*) precipitation and observed All-India Precipitation (AIR—*dashed black line*) time series are correlated with observed Nino3.4 SST index. Correlations are calculated using a 5 month sliding window

in the eastern Pacific where warm water is located north of the equator and cold water is present along the west coast of South America. This north–south irregularity is important for the formation of the annual cycle (Xie 1994) and ENSO (Cane et al. 1986). CCSM4 SST patterns, showed almost the same climatology but with significant differences in magnitude. Figure 16 shows the difference between the simulated CCSM4 SST climatology and the observed SST climatology for DJF, MAM, JJA and SON seasons. In CCSM4, the model predicts warm SSTs over most of the Pacific and Indian Oceans in all four seasons whereas over the eastern equatorial pacific and northern East Indian Ocean, the model has cold SST biases in spring and summer. The cold SST bias in the equatorial Pacific significantly reduces the temperature of the warm pool whereas the warm biases near the coast of Peru reduce the meridional SST gradient. This may be the cause of the double ITCZ in the CCSM4 simulations, as seen in Fig. 12b. Comparing the SST bias in summer with the summer precipitation bias of CCSM4 (Fig. 12) reveals that the negative precipitation anomalies over much of the Pacific Ocean are largely associated with the cold SST bias in the same region. This most likely originates from errors in the atmospheric model. As reported in Li and Hogan (1999), Manganello and Huang (2008), deficiencies in the simulated SSTs are likely responsible for some of the unrealistic ENSO properties in the coupled model. Although CCSM4 simulated summer monsoon precipitation in South Asia is considerably improved, the SST bias over the Pacific Ocean (ENSO region) can still lead to a spurious response of the SAM to ENSO in CCSM4.

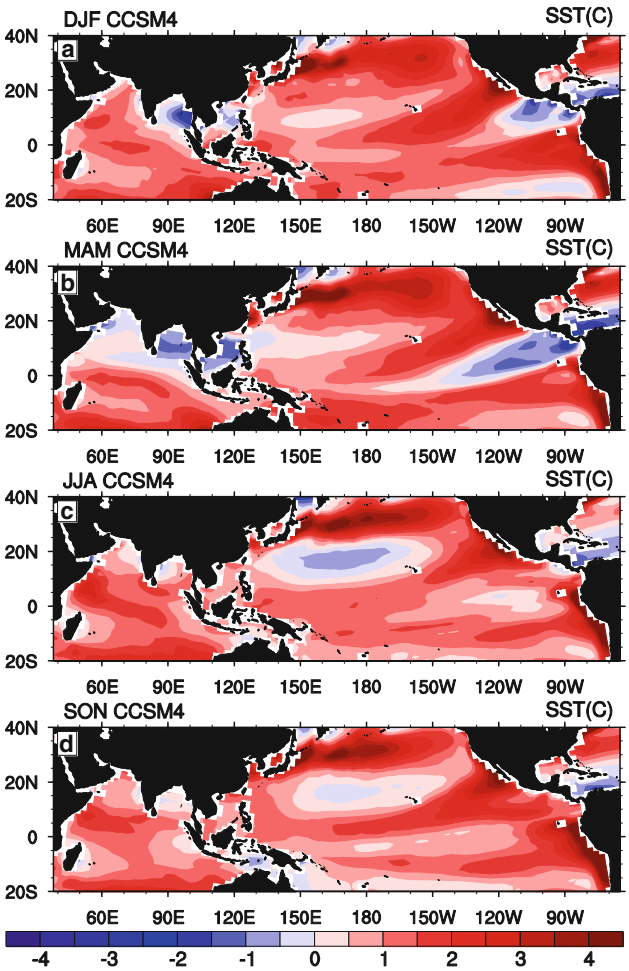

Fig. 16 Seasonal SST differences between CCSM4 and observation (HadSST) for a 30 year mean climatology during: **a** December–February (DJF), **b** March–May (MAM), **c** June–August JJA and **d** September–November (SON). The *shading* corresponds to model SST bias in °C (*red* for warm SST and *blue* for cold SST)

5 The contribution of air sea interaction to SAM simulation

In previous sections, we investigated the SAM simulations using CAM4 and CCSM4. Their differences were due to two factors: (1) the role of coupling in CCSM4 which is absent in CAM4; (2) the SST consistency in CCSM4. To better isolate the role of coupling in simulating the SAM, we designed another set of experiments referred as to CAM4_POP, in which the predicted SST by CCSM4 forces CAM4. These experiments allow us to investigate the air sea coupling in CCSM4 and its effect on SAM precipitation. An ensemble strategy is used as discussed in Sect. 2.2, and therefore the following discussions are from the ensemble mean analysis.

The difference between the CAM4_POP and CCSM4 (Fig. 17b) reveals that the precipitation and westerly winds in the CAM4_POP simulation are enhanced over the Northern Indian Ocean including the Arabian Sea and Bay of Bengal. These differences show that SAM monsoon variability is amplified in the absence of the air–sea coupling. A considerable increase is also seen in the variance (not shown here), revealing that the monsoon variability is amplified by about half as compared with the CCSM4. The absence of the air–sea coupling keeps SSTs warm in the Indian Ocean (as discussed previously), which increases the local evaporation and precipitation. This suggests that the air–sea coupling works to stabilize the monsoon and hence suppress the variability, which is the case in CCSM4 simulations. Figure 17a shows the difference between the CAM4_POP mean precipitation and wind (JJAS), and observations (CMAP/NCEP). The spatial pattern in this case is almost same as seen in Fig. 12b for the SAM region. This means that the reduction in excessive precipitation seen in the CCSM4 simulation is not only due to the air–sea interaction but also due to the more consistent SST simulation in the coupled model integration. In other words, the more consistent SST simulated in CCSM4

(different from observation in magnitude) is responsible for decreasing the overestimation of precipitation.

To further elaborate this point we performed another set of experiments and analyzed the CCSM4 SST in the Indian Ocean and its effect on SAM monsoon. For this set of experiments, we used the SST data from the CCSM4 transient run (CCSM_TR). The CCSM4_TR precipitation is similar to precipitation in the CCSM4 run, but the SST bias is more significant in CCSM4_TR simulation.

The Indian Ocean SST bias, seen in Fig. 16, prompted us to find its influence on the SAM. Comparison of CCSM4 and CAM4 runs suggests that the coupled model cold SST biases significantly reduce monsoon precipitation as seen in Fig. 17. The role of these biases is for CCSM4 to remove the overestimation (reduction in the monsoon) seen in the CAM4 simulation. Gimeno et al. (2010) have shown the Northern Indian Ocean to be an important moisture source for Indian monsoon precipitation and therefore understanding the monsoon dependence on Indian Ocean SST, and correctly representing this in climate models, is important in order to realistically predict monsoon fluctuations.

In Fig. 18a, b, the annual cycle of SST over the Northern Indian Ocean for two separate regions, the Arabian Sea and Bay of Bengal, is shown for observation and for both the CCSM4 and CCSM4_TR coupled model runs. In CCSM4, the magnitude of the cold SST bias in the Arabian Sea is small, diminishing after the summer season, whereas CCSM4_TR shows a large cold bias throughout the year, with a slight decrease in its magnitude during the fall. Over the Bay of Bengal, instead of a cold SST bias, both models show a warm SST bias, with a larger bias in the CCSM4 climatology run. This means, from January to July, the cold bias becomes more confined to the Arabian Sea in these models, while a warming appears in the Bay of Bengal.

To further analyze the role of this Indian Ocean bias, we designed two different sensitivity experiments with CAM4

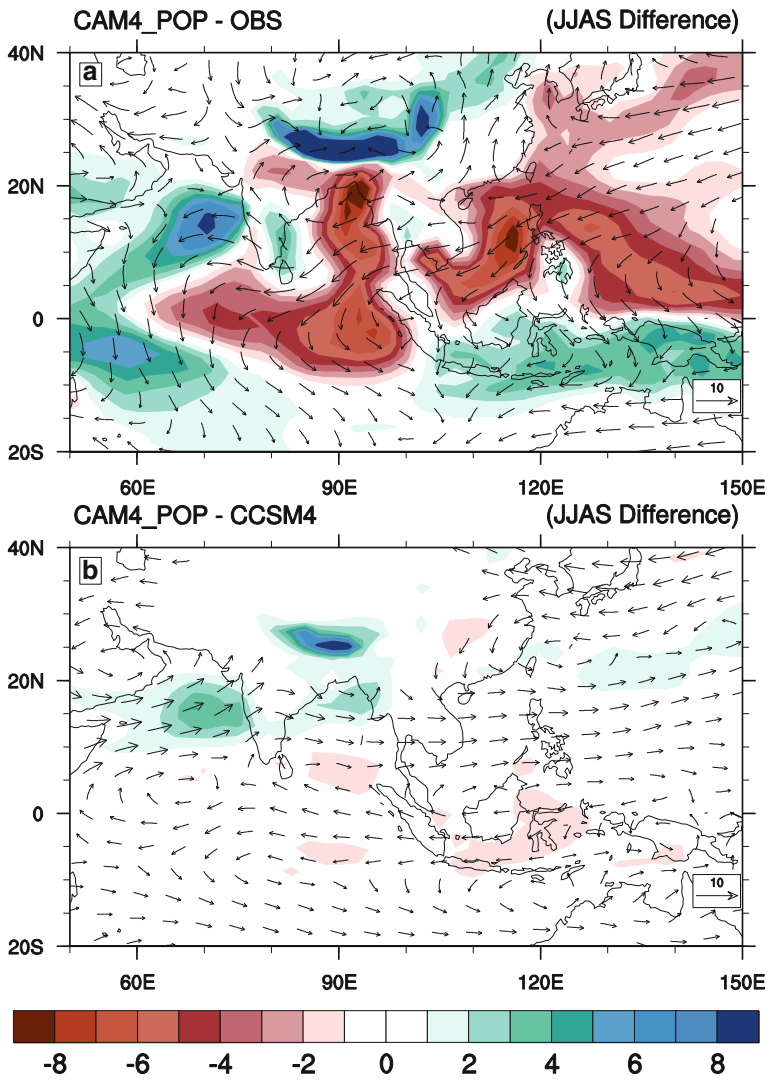

Fig. 17 June–September (JJAS) differences of **a** CAM4_POP (simulation forced with the predicted SST of CCSM4) from observation (CMAP/NCEP) and **b** from CCSM4. *Shading* corresponds to the difference in mm/day whereas vector represents 850 mb winds in m/s

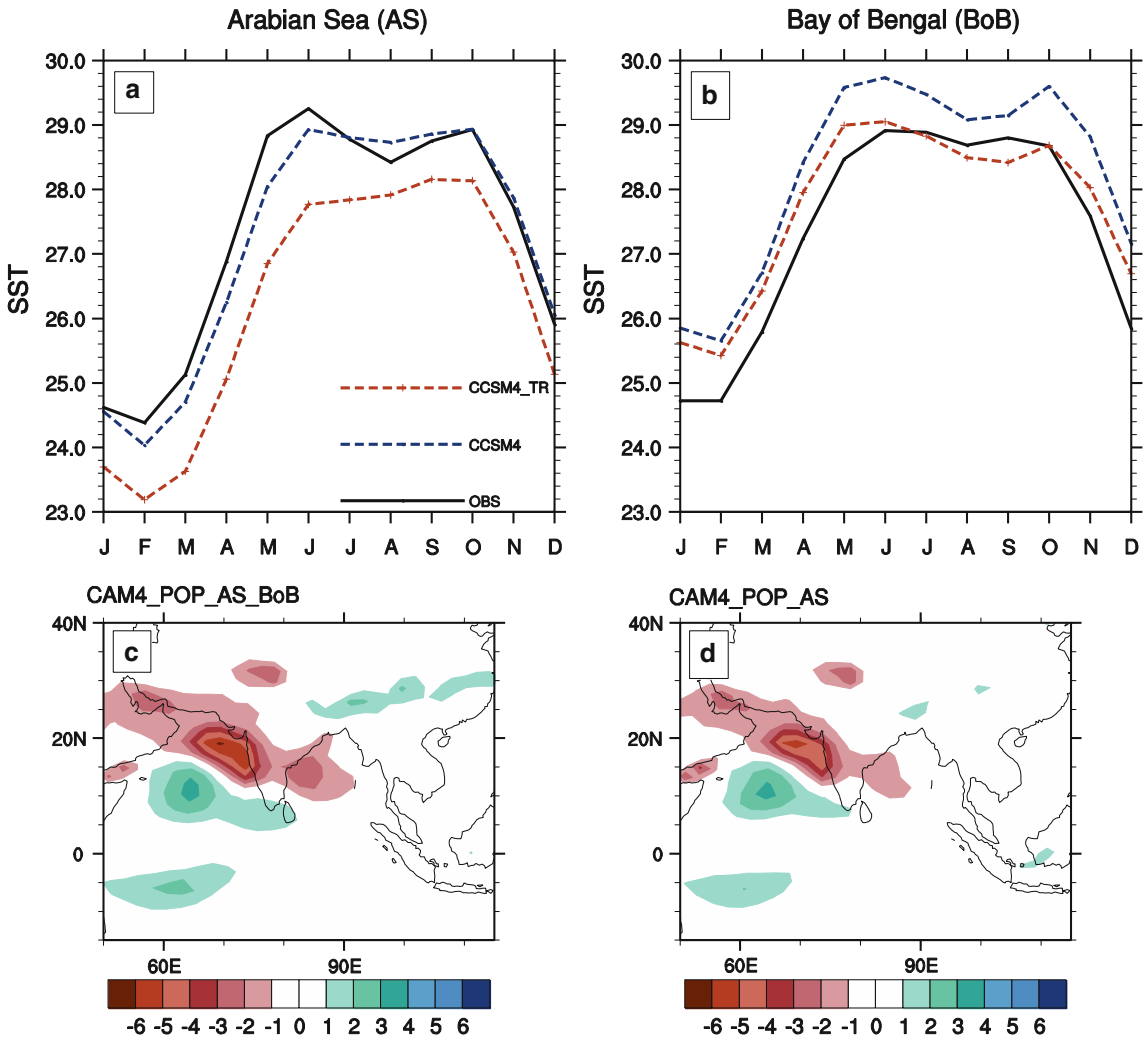

Fig. 18 Annual cycle of observed SST (HadSST, *solid black line*) and simulated SST (CCSM4, *blue dotted line* and CCSM4_TR, *red dotted line*) over **a** Arabian Sea (40°–80°E, 7°–30°N) and **b** Bay of Bengal (80°–100°E, 7°–30°N). **c** June–September (JJAS) mean precipitation difference of CAM4_AS_BoB (CAM4 climatology SST run with SST modification in both Arabian Sea and Bay of Bengal) from CAM4_CLIM (CAM4 climatology SST run). **d** Same as **c** but for CAM4_AS run (with SST modification in Arabian Sea only). The *shading* corresponds to the difference in mm/day

using climatological SST repeated every year but with the addition of the CCSM4 Northern Indian Ocean SST bias into the SST climatology. In the first experiment, we added the annual cycle of CCSM4_TR SST bias (bounded in the Ocean region 7°–30°N, 40°–100°E) covering the whole Northern Indian Ocean to the annual cycle of climatological SST (named as CAM4_AS_BoB). To remove any discontinuity at the boundary of the region of bias the bias is added in a tapered manner over the region, being highest at the center and approaching zero at its boundaries. In the second set of the experiments, the bias of CCSM4_TR SST is confined only to the Arabian Sea covering 7°–30°N, 40°–80°E (named as CAM4_AS). Both of these experiments are compared against the CAM4 climatology run (CAM4_-CLIM) forced with the climatological SST cycle (see Table 1 for details). To account for uncertainties, each simulation is performed three times starting with three different initial conditions. As mentioned previously, CAM4 is not very sensitive to the small changes in its boundary conditions which mean that only a strong anomaly added to its boundary condition will produce a significantly altered simulation. We therefore use the CCSM4_TR simulated SST in this case which has larger magnitude of SST bias, especially in the Arabian Sea. In Fig. 18c, d, precipitation differences of both of these experimental setups from the CAM4_CLIM run are shown. In CAM4_AS_BoB, a significant reduction in the precipitation is seen over the whole Indian subcontinent, Arabian Sea and Bay of Bengal. Also the increased precipitation is seen over the West Indian Ocean around 10°N. In the second experiment (CAM4_AS) where we used the SST bias only over the Arabian Sea, the reduced precipitation

over the Bay of Bengal vanished and only the Arabian Sea is affected by the bias. Both these experiments support our conclusion that the reduction of CCSM4 SAM precipitation is mainly due to the SST bias in Northern Indian Ocean. The weakened (reduced precipitation as compared to CAM4) monsoon seen in the CCSM4 run is therefore mainly caused by systematic cold SST biases of Northern Indian Ocean particularly in the Arabian Sea. This cold bias keeps the ocean cool, and thus reduces evaporation, which results into the reduction of SAM precipitation. This issue needs more attention in the coupled model to improve monsoon simulation. CCSM4, while being revised with improved physics and dynamics, needs improvement in its oceanic counterpart.

6 Summary and conclusions

The SAM precipitation is an important climatic feature due to its profound influence on droughts and floods over Asia, along with its influence on the global general circulation. Improved and accurate simulation of the SAM system is therefore crucial to predict decadal and seasonal climate as well as projecting long-term climate change in the region. Also it is necessary to assess whether climate models can realistically simulate monsoon systems before using them for such predictions. This study discussed selected features of the SAM precipitation in the simulations of NCAR's new versions of the uncoupled (CAM) and coupled (CCSM) climate models. Simulations using CAM4, CAM5 and CCSM4 models are performed and compared against observations to identify improvements and discrepancies in these newly updated models. Along with the simulated mean climatology of the region, the interannual variability and SAM–ENSO/IOD teleconnections are evaluated using lag-lead correlation and regression analysis. The improvements due to air–sea interactions and impact of SST biases from the CCSM4 are assessed in coupled model simulations.

It is found, in the comparison of atmosphere-only simulations, that the improvements in CAM4 and CAM5 dynamics and convection parameterizations have eliminated many regional differences (specially for CAM5). Many improvements in these simulations, compared to previous versions, are seen in both models. The detailed structure of spatial patterns and the seasonal cycle of monsoon precipitation are well reproduced in both CAM4 and CAM5. The annual cycle of average precipitation is well simulated along with it major characteristics such as the rapid monsoon onset between May and June, the high precipitation during June–August and slow withdrawal during September–October. The large northward shift of the ITCZ from January to July is also well simulated by both CAM4 and CAM5 and its location and strength are fairly well reproduced. Increasing the resolution shows a pronounced improvement in precipitation simulation with a reduction in many regional biases, especially over regions of complex terrain. The CAM5 new dynamics and physics showed improved simulation results over the SAM region. Sensitivity experiments using CAM5 showed that the implementation of new boundary layer schemes (UW moist turbulence) in CAM5 contributes to decreasing the CAM4 simulation overestimation.

Analysis showed that both CAM4 and CAM5 poorly simulate the ENSO–monsoon teleconnection. These models partially captured the monsoon interannual variability with inconsistencies in oscillatory period and amplitude. It is also found that the simulation of East Asian summer monsoon is much better than the simulation of the SAM in both CAM4 and CAM5. The better simulation of the WY and WNPM monsoon indices and poor simulation of the IM, SAM_i and ISR monsoon indices in both CAM4 and CAM5 also supported this conclusion. Both the models are able to simulate the wind circulation such as equatorial monsoon flow and lower level jet stream very well. Both models simulate excessive precipitation over the western Indian Ocean and subtropical Pacific Ocean whereas decreased precipitation is simulated over the eastern Indian Ocean, China Sea and South America. Over the SAM region their simulations show significant large-scale biases such as excessive precipitation over the Arabian bay and over the Western Ghats of India, and reduced precipitation over the eastern Indian Ocean extending into the Bay of Bengal.

The CCSM4 simulated SAM precipitation is considerably improved compared with CAM4 with the reduction of many biases particularly over the Arabian Peninsula and the western coast of India. The results showed that the air–sea coupling has significantly improved the monsoon simulation. Along with these improvements, interrupted northward progression and delayed onset of the monsoon over the SAM region is seen. The CCSM4 underestimated the precipitation over the equatorial area in the Pacific Ocean. Also CCSM4 still has the double ITCZ problem that was also present in the previous versions of the CCSM model (CCSM3). CCSM4 showed a systematic cold bias in the simulation of SSTs over the tropical Pacific Ocean and hence showed problems in simulating the observed SST–precipitation relationship. Analysis over the whole tropical region revealed that biases in CAM4 and CCSM4 are somewhat similar to those in previous versions of these models.

The frequency of ENSO in CCSM4 is found to be more realistic than was simulated in its previous version (CCSM3). The SAM–ENSO teleconnection in the CCSM4 climatology run is partially captured. Significant cold

biases over the equatorial Pacific Ocean are found in CCSM4, particularly in winter and early summer. It is seen that the air–sea coupling can improve the simulation of precipitation. Forcing CAM4 with coupled model SST clarified the impact of the air–sea coupling in the interannual variability of the SAM precipitation. The local air–sea coupling over the SAM region acts to modulate the activity of the SAM summer monsoon as well as the remote SST forcing. The SST continuously warms over the SAM region as the feedback from the atmosphere to the ocean does not exist in the CAM4 model forced with SST from the coupled model. The SST warming contributes to increased evaporation, which results in the monsoon destabilization over the SAM region. Another impact, the absence of the air–sea coupling, enhances heavier precipitation in the SAM. It is found that, along with air–sea interaction, SST bias in the CCSM4 model plays an important role in simulation of SAM precipitation variability and magnitude. Using CAM4 sensitivity experiments, the influence of the coupled model SST bias in the northern Indian Ocean on SAM precipitation is investigated. It is found that the reduction of SAM precipitation in the coupled simulation, as compared to the uncoupled simulation, is mainly due to cold SST bias in the Arabian Sea.

The strengths and limitations in simulating Asian summer monsoon in CAM4, CAM5 and CCSM4, depend mainly on how well they simulate the mean state of atmosphere, its variability, the internal dynamics of monsoon systems and ocean–atmosphere interactions. Although these recent model versions have many improvements and are able to capture the observed features of SAM precipitation, many biases are still present. This study shows that while the NCAR systems models can serve as tools in simulating and understanding Asian monsoon climate systems, they still have simulation errors that need further consideration. Along with the improvements in the model physics and resolution, understanding of the coupled physical processes in conjunction with the complex topography over the SAM region is crucial. As the ocean dynamics also play an important role in Indian Ocean SST, further studies are needed to clarify its relative importance compared with the role of air–sea interaction in SST cooling during the SAM. It is necessary for the coupled model to simulate realistic SST variation to improve the SST climatology, which can then improve the SAM precipitation teleconnection in CCSM4. In general, modeling monsoon fluctuations mainly depends on understanding the fundamental processes that affect local climate, good parameterization and representation of these processes and the methods used for numerical implementation of these processes.

Acknowledgments This work is supported by Canadian Foundation for Climate and Atmospheric Sciences (CFCAS) under research grant GR-7027. The authors are thankful to NCAR for providing models and their input data sets as well as providing assistance during simulations. We are also grateful for the comments provided by anonymous reviewers, which helped us improve and clarify the paper.

References

AchutaRao KM, Sperber KR (2006) ENSO simulation in coupled ocean–atmosphere models: are the current models better? Clim Dyn 27:1–15. doi:10.1007/s00382-006-0119-7

Anderson J, Hoar T, Raeder K, Liu H, Collins N, Torn R, Avellano A (2009) The data assimilation research testbed: a community facility. Bull Am Meteorol Soc 90:1283–1296

Annamalai H, Liu P (2005) Response of the Asian summer monsoon to changes in El Niño properties. Q J R Meteorol Soc 131: 805–831

Annamalai H, Hamilton K, Sperber KR (2007) South Asian summer monsoon and its relationship with ENSO in the IPCC AR4 simulations. J Clim 20:1071–1092. doi:10.1175/JCLI4035.1

Cane MA, Zebiak SE, Dolan SC (1986) Experimental forecasts of El Niño. Nature 321:827–832

Chung C, Nigam S (1999) Asian summer monsoon-ENSO feedback on the Cane–Zebiak model ENSO. J Clim 12:2787–2807

Collins WD et al (2006a) The Community Climate System Model version 3 (CCSM3). J Clim 19:2122–2143

Collins WD et al (2006b) The formulation and atmospheric simulation of the Community Atmosphere Model: CAM3. J Clim 19:2144–2161

Covey C, AchutaRao KM, Lambert SJ, Taylor KE (2000) Intercomparison of present and future climates simulated by coupled ocean–atmosphere GCMs. PCMDI report no 66. Program for climate model diagnosis and intercomparison, Lawrence Livermore National Laboratory. University of California, Livermore

Covey C, AchutaRao KM, Cubasch U, Jones P, Lambert SJ, Mann ME, Phillips TJ, Taylor KE (2003) An overview of results from the coupled model intercomparison project (CMIP). Glob Planet Chang 37:103–133. doi:10.1016/S0921-8181(02)00193-5

Dai A (2006) Precipitation characteristics in eighteen coupled climate models. J Clim 19:4605–4630. doi:10.1175/JCLI3884.1

Gadgil S, Sajani S (1998) Monsoon precipitation in the AMIP runs. Clim Dyn 14:659–689

Gent PR et al (2011) The Community Climate System Model version 4. J Clim 24:4973–4991. doi:10.1175/2011JCLI4083.1

Gimeno L, Drumond A, Nieto R, Trigo RM, Stohl A (2010) On the origin of continental precipitation. Geophys Res Lett 37:L13804. doi:10.1029/2010GL043712

Goswami BN, Krishnamurthy V, Annamalai H (1999) A broad-scale circulation index for the interannual variability of the Indian summer monsoon. Q J R Meteorol Soc 125:611–633

Hack JJ, Kiehl JT, Hurrell JW (1998) The hydrologic and thermodynamic characteristics of the NCAR CCM3. J Clim 11:1179–1206

Holtslag A, Boville B (1993) Local versus nonlocal boundary-layer diffusion in a global climate model. J Clim 6:1825

Hunke EC, Lipscomb WH (2008) CICE: the Los Alamos sea ice model user's manual, version 4. Los Alamos National Laboratory technical report LA-CC-06-012

Iacono MJ, Delamere J, Mlawer E, Shephard M, Clough S, Collins W (2008) Radiative forcing by long-lived greenhouse gases: calculations with the AER radiative transfer models. J Geophys Res 113:D13103. doi:10.1029/2008JD009944

IPCC (2007) Climate change 2007—the physical science basis. In: Solomon S, Qin D, Manning M, Chen Z, Marquis M, Averyt KB, Tignor M, Miller HL (eds) Contribution of working group I to the fourth assessment report of the Intergovernmental Panel on Climate Change. Cambridge University Press, Cambridge

Joseph R, Nigam S (2006) ENSO evolution and teleconnections in IPCC's twentieth-century climate simulations: realistic representation? J Clim 19:4360–4377. doi:10.1175/JCLI3846.1

Kanamitsu M, Krishnamurti TN (1978) Northern summer tropical circulation during drought and normal rainfall months. Mon Weather Rev 106:331–347

Kang IS, Shukla J (2006) Dynamic seasonal prediction and predictability (Chap. 15). The Asian monsoon. Springer Praxis, Chichester, pp 585–612

Kang IS et al (2002) Intercomparison of the climatological variations of Asian summer monsoon precipitation simulated by 10 GCMs. Clim Dyn 19:383–395

Kang IS, Lee JY, Park CK (2004) Potential predictability of summer mean precipitation in a dynamical seasonal prediction system with systematic error correction. J Clim 17:834–844

Kiehl JT, Gent PR (2004) The Community Climate System Model, version 2. J Clim 17:3666–3682

Kirtman BP, Shukla J (2000) Influence of the Indian summer monsoon on ENSO. Q J R Meteorol Soc 126:213–239

Kistler R, Kalnay E, Collins W et al (2001) The NCEP-NCAR 50-year reanalysis: monthly means CD-ROM and documentation. AMS Bull 82:247–267

Kitoh A, Arakawa O (1999) On overestimation of tropical precipitation by an atmospheric GCM with prescribed SST. Geophys Res Lett 26:2965–2968

Kripalani RH, Oh JH, Kulkarni A, Sabade SS, Chaudhari HS (2007) South Asian summer monsoon precipitation variability: coupled climate model simulations and projections under IPCC AR4. Theor Appl Climatol 90:133–159. doi:10.1007/s00704-006-0282-0

Krishnamurti TN, Bedi HS, Subramaniam M (1989) The summer monsoon of 1987. J Clim 2:321–340

Kumar K, Hoerling M, Rajagopalan B (2005) Advancing dynamical predictions of the Indian monsoon rainfall. Geophys Res Lett 32:L08704. doi:10.1029/2004GL021979

Lal M, Bengtsson L, Cubash U, Esch M, Schlese U (1995) Synoptic scale disturbances of the Indian summer monsoon as simulated in a high resolution climate model. Clim Res 5:243–258

Lau KM, Li MT (1984) The monsoon of East Asia and its global associations—a survey. Bull Am Meteorol Soc 65:114–125

Lee JY, Wang B, Kang IS, Shukla J et al (2010) How are seasonal prediction skills related to models' performance on mean state and annual cycle? Clim Dyn. doi:10.1007/s00382-010-0857-4

Li T, Hogan TF (1999) The role of the annual-mean climate on seasonal and interannual variability of the tropical Pacific in a coupled GCM. J Clim 12:780–792

Liang J, Yang S, Hu ZZ, Huang B, Kumar A, Zhang Z (2009) Predictable patterns of the Asian and Indo-Pacific summer precipitation in the NCEP CFS. Clim Dyn 32:989–1001

Lin JL (2007) The double-ITCZ problem in IPCC AR4 coupled GCMs: ocean–atmosphere feedback analysis. J Clim 20:4497–4525. doi:10.1175/JCLI4272.1

Liu X, Easter RC, Ghan SJ, Zaveri R, Rasch P, Shi X, Lamarque J-F, Gettelman A, Morrison H, Vitt F, Conley A, Park S, Neale R, Hannay C, Ekman AML, Hess P, Mahowald N, Collins W, Iacono MJ, Bretherton CS, Flan-ner MG, Mitchell D (2012) Toward a minimal representation of aerosols in climate models: description and evaluation in the Community Atmosphere Model CAM5. Geosci Model Dev 5:709–739. doi:10.5194/gmd-5-709-2012

Malik N, Marwan N, Kurths J (2010) Spatial structures and directionalities in monsoonal precipitation over south Asia. Nonlinear Process Geophys 17:371–381

Manganello JV, Huang B (2008) The influence of systematic errors in the Southeast Pacific on ENSO variability and prediction in a coupled GCM. Clim Dyn. doi:10.1007/s00382-008-0407-5

Meehl GA, Arblaster JM (1998) The Asian–Australian monsoon and El Nino–Southern Oscillation in the NCAR climate system model. J Clim 11:1356–1385

Meehl GA, Arblaster JM (2002) Indian monsoon GCM sensitivity experiments testing tropospheric biennial oscillation transition conditions. J Clim 15:923–944

Meehl GA, Covey C, McAvaney B, Latif M, Stouffer RJ (2005) Overview of the coupled model intercomparison project. Bull Am Meteorol Soc 86:89–93. doi:10.1175/BAMS-86-1-89

Meehl GA, Arblaster JM, Lawrence DM, Seth A, Schneider EK, Kirtman BP, Min D (2006) Monsoon regimes in the CCSM3. J Clim 19:2482–2495

Meehl GA, Arblaster JM, Caron JM, Annamalai H, Jochum M, Chakraborty A, Murtugudde R (2012) Monsoon regimes and processes in CCSM4. Part I: the Asian–Australian monsoon. J Clim 25(8):2583–2608. doi:10.1175/JCLI-D-11-00184.1

Morrison H, Gettelman A (2008) A new two-moment bulk 688 stratiform cloud micro physics scheme in the NCAR Community Atmosphere Model (CAM3), part I: description and numerical tests. J Clim 21:3642–3659

Neale RB, Jochum M, Richter JH (2008) The impact of convection on ENSO: from a delayed oscillator to a series of events. J Clim 21:5904–5924

Neale RB et al (2010a) Description of the NCAR Community Atmosphere Model (CAM 4.0). NCAR technical note NCAR/TN-485+STR, National Center for Atmospheric Research, Boulder

Neale RB et al (2010b) Description of the NCAR Community Atmosphere Model (CAM 5.0). NCAR technical note NCAR/TN-486+STR, National Center for Atmospheric Research, Boulder

Palmer TN, Brankovic C, Viterbo P, Miller MJ (1992) Modelling interannual variations of summer monsoons. J Clim 5:399–417

Pant GB, Parthasarathy B (1981) Some aspects of an association between the southern oscillation and Indian summer monsoon. Arch Meteorol Geophys Bioklimatol B 29:245–251

Park S, Bretherton CS (2009) The University of Washington shallow convection and moist turbulence schemes and their impact on climate simulations with the Community Atmosphere Model. J Clim 22:3449–3469

Parthasarathy B, Munot AA, Kothawale DR (1995) All India monthly and seasonal rainfall series: 1871–1993. Theor Appl Climatol 49:217–224. doi:10.1007/BF00867461

Randall DA, Wood RA, Bony S, Colman R, Fichefet T, Fyfe J, Kattsov V, Pitman A, Shukla J, Srinivasan J, Stouffer RJ, Sumi A, Taylor KE (2007) Climate models and their evaluation. In: Climate change 2007: the physical science basis. Contribution of working group I to the fourth assessment report of the Intergovernmental Panel on Climate Change. Cambridge University Press, Cambridge

Rasmusson EM, Carpenter TH (1983) The relationship between eastern equatorial Pacific sea surface temperature and surface wind fields associated with the Southern Oscillation/El Niño. Mon Weather Rev 111:517–528

Reynolds RW, Rayner NA, Smith TM, Stokes DC, Wang W (2002) An improved in situ and satellite SST analysis for climate. J Clim 15:1609–1625

Richter J, Rasch P (2008) Effects of convective momentum transport on the atmospheric circulation in the Community Atmosphere Model, version 3. J Clim 21:1487–1499

Rowell DP, Folland CK, Maskell K, Ward MN (1995) Variability of summer rainfall over tropical North Africa (1906–92): observations and modelling. Q J R Meteorol Soc 121:669–674

Saji NH, Goswami BN, Vinayachandran P, Yamagata T (1999) A dipole mode in the tropical Indian ocean. Nature 401:360–363

Shukla J, Mooley DA (1987) Empirical prediction of the summer monsoon rainfall over India. Mon Weather Rev 115:695–703

Shukla J, Paolino DA (1983) The Southern Oscillation and long-range forecasting of the summer monsoon rainfall over India. Mon Weather Rev 111:1830–1837

Sikka DR (1999) Monsoon drought in India. Joint COLA/CARE technical report no. 2. Center for Ocean–Land–Atmosphere Studies and Center for the Application of Research on the Environment, 93 pp

Smith RD, Gent P (2002) Reference manual for the Parallel Ocean Program (POP). Los Alamos unclassified report LA-UR-02-2484

Smith RD, Kortas S (1995) Curvilinear coordinates for global ocean models. Los Alamos unclassified report LA-UR-95-1146

Vavrus S, Waliser D (2008) An improved parameterization for simulating Arctic cloud amount in the CCSM3 climate model. J Clim 21:5673–5687

Waliser D, Seo KW, Schubert S, Njoku E (2007) Global water cycle agreement in the climate models assessed in the IPCC AR4. Geophys Res Lett 34:L16705. doi:10.1029/2007GL030675

Wang B, Fan Z (1999) Choice of South Asian summer monsoon indices. Bull Am Meteorol Soc 80:629–638

Wang B, Wu R, Lau KM (2001) Interannual variability of the Asian summer monsoon: contrasts between the Indian and the western North Pacific-East Asian monsoons. J Clim 15:4073–4090

Wang B, Kang IS, Li JY (2004) Ensemble simulation of Asian–Australian monsoon variability by 11 AGCMs. J Clim 17:803–818

Wang B, Ding QH, Fu XH, Kang I-S, Jin K, Shukla J, Doblas-Reyes F (2005) Fundamental challenge in simulation and prediction of summer monsoon rainfall. Geophys Res Lett 32:L15711

Webster PJ, Yang S (1992) Monsoon and ENSO: selectively interactive systems. Q J R Meteorol Soc 118:877–926

Wu X, Liang X, Zhang GJ (2003) Seasonal migration of ITCZ precipitation across the equator: why can't GCMs simulate it? Geophys Res Lett 30(15):1824–1828

Xie SP (1994) On the genesis of the equatorial annual cycle. J Clim 7:2008–2013

Xie P, Arkin PA (1997) Global precipitation: a 17-year monthly analysis based on gauge observations, satellite estimates, and numerical model outputs. Bull Am Meteorol Soc 78:2539–2558

Yasunari T (1990) Impact of Indian monsoon on the coupled atmosphere/ocean systems in the tropical Pacific. Meteorol Atmos Phys 44:29–41